

# Atmospheric conditions and composition that influence PM<sub>2.5</sub> oxidative potential in Beijing, China

Steven J. Campbell<sup>1,2\*</sup>, Kate Wolfer<sup>1\*</sup>, Battist Uttinger<sup>1</sup>, Joe Westwood<sup>2</sup>, Zhi-hui Zhang<sup>1,2</sup>, Nicolas Bukowiecki<sup>1</sup>, Sarah S. Steimer<sup>2§</sup>, Tuan V. Vu<sup>3#</sup>, Jingsha Xu<sup>3</sup>, Nicholas Straw<sup>4</sup>, Steven Thomson<sup>3</sup>, Atallah Elzein<sup>5</sup>, Yele Sun<sup>6</sup>, Di Liu<sup>3,6</sup>, Linjie Li<sup>6</sup>, Pingqing Fu<sup>8</sup>, Alastair C. Lewis<sup>5,7</sup>, Roy M. Harrison<sup>3†</sup>, William J. Bloss<sup>3</sup>, Miranda Loh<sup>9</sup>, Mark R. Miller<sup>4</sup>, Zongbo Shi<sup>3</sup> and Markus Kalberer<sup>1,2</sup>

<sup>1</sup>Department of Environmental Sciences, University of Basel, Basel, Switzerland

<sup>2</sup>Department of Chemistry, University of Cambridge, Cambridge, UK

<sup>3</sup>School of Geography Earth and Environmental Sciences, University of Birmingham, Birmingham, UK

<sup>4</sup>Centre for Cardiovascular Science, Queen's Medical Research Institute, University of Edinburgh, Edinburgh, UK

<sup>5</sup>Wolfson Atmospheric Chemistry Laboratories, Department of Chemistry, University of York, York, UK

<sup>6</sup>State Key Laboratory of Atmospheric Boundary Layer Physics and Atmospheric Chemistry, Institute of Atmospheric Physics, Chinese Academy of Sciences, Beijing, China

<sup>7</sup>National Centre for Atmospheric Science, University of York, York, UK

<sup>8</sup>Institute of Surface Earth System Science, Tianjin University, Tianjin, China

<sup>9</sup>Institute of Occupational Medicine, Edinburgh, UK

<sup>§</sup> Now at: Department of Environmental Science, Stockholm University, Stockholm, Sweden

<sup>†</sup> Also at: Department of Environmental Sciences / Center of Excellence in Environmental Studies, King Abdulaziz University, PO Box 80203, Jeddah, 21589, Saudi Arabia

<sup>#</sup> Now at School of Public Health, Imperial College London, London, UK

\*Authors contributed equally to the manuscript

Correspondence to: stevenjohn.campbell@unibas.ch

**Abstract.** Epidemiological studies have consistently linked exposure to PM<sub>2.5</sub> with adverse health effects. The oxidative potential (OP) of aerosol particles has been widely suggested as a measure of their potential toxicity. Several acellular chemical assays are now readily employed to measure OP, however, uncertainty remains regarding the atmospheric conditions and specific chemical components of PM<sub>2.5</sub> that drive OP. A limited number of studies have simultaneously utilised multiple OP assays with a wide range of concurrent measurements and investigated the seasonality of PM<sub>2.5</sub> OP. In this work, filter samples were collected in winter 2016 and summer 2017 during the atmospheric pollution and human health in a Chinese megacity (APHH-Beijing) campaign, and PM<sub>2.5</sub> OP was analysed using four acellular methods; ascorbic acid (AA), dithiothreitol (DTT), 2-7-dichlorofluoroscine/hydrogen peroxidase (DCFH) and electron paramagnetic resonance spectroscopy (EPR). Each assay reflects different oxidising properties of PM<sub>2.5</sub>, including particle-bound ROS (DCFH), superoxide radical production (EPR) and catalytic redox chemistry (DTT/AA), and combination of these four assays provided a detailed overall picture of the oxidising properties of PM<sub>2.5</sub> at a central site in Beijing. Positive correlations of OP (normalised per volume of air) of all four

assays with overall PM<sub>2.5</sub> mass was observed, with stronger correlations in ~~the~~ winter compared to ~~the~~ summer. In contrast, when OP assay values were normalised for particle mass, days with higher PM<sub>2.5</sub> mass concentrations ( $\mu\text{g m}^{-3}$ ) were found to have lower ~~intrinsic~~ mass-normalised OP values as measured by AA and DTT. This ~~indicates~~finding supports that total PM<sub>2.5</sub> mass concentrations alone ~~might~~may not always be the best indicator for particle toxicity. Univariate analysis of OP values and an extensive range of additional measurements, 107 in total, including PM<sub>2.5</sub> composition, gas phase composition and meteorological data, ~~provides~~provided detailed insight into the chemical components ~~of~~and atmospheric processes that determine PM<sub>2.5</sub> OP variability. Multivariate statistical analyses highlighted associations of OP assay responses with varying chemical components in PM<sub>2.5</sub> for both mass- and volume-normalised data. ~~Variable selection was used to produce subsets of measurements indicative of PM<sub>2.5</sub> sources, and used to model OP response;~~ AA and DTT assays were well predicted by a small panel~~set~~ of measurements in multiple linear regression (MLR) models, and indicated fossil fuel combustion ~~processes~~, vehicle emissions and biogenic SOA as ~~most~~-influential particle sources in the assay response. ~~Through comparative~~Mass MLR models of OP associated with compositional source profiles predicted OP almost as well as volume MLR models, illustrating the influence of mass composition on both particle-level OP and total volume OP. Univariate and multivariate analysis showed that different assays cover different chemical spaces, and through comparison of both mass- and volume-normalised data we also demonstrate ~~the utility of considering that mass-normalised OP when correlating with particle composition measurements, which provides a more nuanced picture of compositional drivers and sources of OP compared to volume-normalised analysis, and which may be more useful in temporal and site comparative contexts. This study constitutes one of the most extensive and comprehensive composition datasets currently available, and provides a unique opportunity to explore chemical variations in PM<sub>2.5</sub> and how they affect both PM<sub>2.5</sub> OP and the concentrations of particle-bound ROS.~~

## 1 Introduction

Large-scale epidemiological studies have consistently linked the exposure of airborne particulate matter (PM) with a range of adverse human health effects (Hart et al., 2015; Laden et al., 2006; Lepeule et al., 2012). A recent study by the World Health Organisation estimated that 1 in 8 deaths globally in 2014 were linked to air pollution exposure (World Health Organisation, 2016) with urban areas in India and China particularly affected (~~Lelieveld et al., 2020~~)(Lelieveld et al., 2020). However, large uncertainty remains regarding the physical and chemical characteristics of PM that result in adverse health outcomes upon exposure (~~Bates et al., 2019~~)(Bates et al., 2019).

Studies have suggested that oxidative stress promoted by PM components *in vivo* could be a key mechanism that results in adverse health outcomes (Donaldson and Tran, 2002; Knaapen et al., 2004; Øvrevik et al., 2015). Oxidative stress occurs when excess concentrations of reactive oxygen species (ROS) overwhelm cellular anti-oxidant defences, resulting in an imbalance of the oxidant-antioxidant ratio in favour of the former, which can subsequently lead to inflammation and disease (Knaapen et al., 2004; Li et al., 2003, 2008). The term ROS typically refers to H<sub>2</sub>O<sub>2</sub>, in some cases including organic peroxides, the hydroxyl radical ( $\cdot\text{OH}$ ), superoxide ( $\text{O}_2^{\cdot-}$ ) and organic oxygen-centred radicals. Particle-bound ROS is exogenously delivered into the

70 lung through PM inhalation, ~~and ROS~~ can be produced *in vivo* via redox-chemistry initiated by certain particle components, in addition to baseline tissue ROS produced by metabolic processes (~~Dellinger et al., 2001~~)(Dellinger et al., 2001). The capability of PM to produce ROS with subsequent depletion of anti-oxidants upon inhalation is defined as oxidative potential (OP) (Bates et al., 2019).

~~OP is a fairly simple measure of PM redox activity, but reflects a complex interplay of particle size, composition and chemistries which induce oxidative stress by free radical generation which triggers cellular signal transduction and damage. These effects can be both localised (to lung epithelial surfaces and alveoli, reviewed by (Tao et al., 2003)) and systemic (through immune system activation and cytokine release (Miyata and van Eeden, 2011), translocation of ultrafine particles into the circulatory system (Oberdorster et al., 1992), increased circulating monocytes (Tan et al., 2000), and propagation to other cells and organs (Laing et al., 2010; Meng and Zhang, 2006). Oxidative stress is implicated in the majority of toxicological effects related to air pollution (Ghio et al., 2012; Kelly, 2003; Pope and Dockery, 2006; Risom et al., 2005). A rapid and simple metric to capture the oxidative exposure burden which can be easily implemented for epidemiological studies will enable greater insight into the mechanisms of PM toxicity beyond total PM mass exposure and the most commonly measured (generally non-redox active) toxic components of PM, such as measures of elemental or organic carbon and PAH concentrations.~~

85 OP is a fairly simple measure of PM redox activity, but reflects a complex interplay of particle size, composition and chemistries which induce oxidative stress by free radical generation which triggers cellular signal transduction and damage. These effects can be both localised (to lung epithelial surfaces and alveoli, reviewed by Tao et al., 2003) and systemic, through immune system activation and cytokine release (Miyata and van Eeden, 2011), translocation of ultrafine particles into the circulatory system (Oberdorster et al., 1992), increased circulating monocytes (Tan et al., 2000), and propagation to other cells and organs (Laing et al., 2010; Meng and Zhang, 2006). Oxidative stress is implicated in the majority of toxicological effects related to air pollution (Ghio et al., 2012; Kelly, 2003; Pope and Dockery, 2006; Risom et al., 2005). A rapid and simple metric to capture the oxidative exposure burden which can be easily implemented for epidemiological studies will enable greater insight into the mechanisms of PM toxicity beyond total PM mass concentrations alone.

90 There are now a wide range of acellular chemical methods that attempt to quantify ~~particle-bound ROS~~ and the entire OP of PM ~~and particle-bound ROS~~, as typically acellular assays allow faster measurement and are less labour intensive compared to cell cultures or *in vivo* methods (~~Bates et al., 2019~~)(Bates et al., 2019). These include, but are not limited to, the dithiothreitol assay (DTT), ascorbic acid assay (AA), 2-7-~~diehlorofluoresee~~indichlorofluoroscine/hydrogen peroxidase assay (DCFH), electron paramagnetic spectroscopy (EPR), glutathione assay (GSH) and 9-(1,1,3,3-tetramethylisindolin-2-yl)oxyl-5-ethynyl)-10-(phenylethynyl)anthracene (BPEAnit). These acellular assays all have differing sensitivities to specific particle components that may contribute to increased particle-bound ROS concentrations and aerosol OP. For instance, DTT has been shown to be sensitive to soluble metals (Shinyashiki et al., 2009), including copper and manganese (Charrier et al., 2015; Charrier and Anastasio, 2012), as well as a range of organic particle components including water soluble organic carbon (WSOC, a mixture of 100's to 1000's of compounds), oxidised polycyclic aromatic hydrocarbons (PAHs) e.g. quinones (Chung et al., 2006;

Field Code Changed

McWhinney et al., 2013a), and humic-like substances (HULIS) (Dou et al., 2015; Verma et al., 2015a). AA is particularly sensitive to redox-active transition metals, most notably Fe (Godri et al., 2011) and Cu (Janssen et al., 2014; Pant et al., 2015), and has demonstrated sensitivity to organic carbon (Calas et al., 2018) including secondary organic aerosol (Campbell et al., 2019b; Campbell et al., 2019a). EPR is applied to speciate and quantify radical species either bound to aerosol particles (Arangio et al., 2016; Campbell et al., 2019a; Gehling and Dellinger, 2013) (Arangio et al., 2016; Campbell et al., 2019b; Gehling and Dellinger, 2013), so-called environmentally persistent free radicals (EPFR), or radicals formed upon suspension of particles into aqueous solution (Gehling et al., 2014; Tong et al., 2016, 2017) or in some cases into synthetic lung lining fluid (Tong et al., 2018) consisting of a mixture of AA, glutathione and uric acid. EPR has the advantage of not being influenced by the dark colour of particulate suspensions (detection is *via* magnetic excitation rather than magnetic absorbance), does not require extraction of the PM from the filter, and that speciation of the free radical generated can be explored using spin-trap reagents that are selective for specific radicals (Miller et al., 2009). The DCFH assay has been shown to be particularly sensitive to hydrogen peroxide (H<sub>2</sub>O<sub>2</sub>) and organic peroxides (Venkatachari and Hopke, 2008; Wragg et al., 2016), also present in secondary organic aerosol (SOA) particles (Gallimore et al., 2017), and is a particularly useful assay for measuring particle-bound ROS (Wragg et al., 2016). The application of these four commonly used assays simultaneously allows different mechanisms of ROS generation to be assessed; the variability of particle-bound ROS (DCFH), the production of superoxide upon aqueous particle suspension (EPR) and the catalytic generation of ROS via redox-active components (DTT/AA). Therefore, these data provide a broad picture of the variability of both particle-bound ROS and OP, and comparison to a comprehensive compositional dataset provides a unique opportunity to probe the chemical changes in PM that affect the burden of particle-bound ROS and OP.

Despite several studies utilising the aforementioned assays, further exploratory work is required to determine specifically ~~what~~which sources, physical properties and chemical components influence aerosol OP variability. A limited ~~amount~~number of studies have explored the role of chemical composition on aerosol OP, and it is often unclear which specific chemical components are responsible for driving aerosol OP; for example, studies show transition metals such as Cu and Mn dominate DTT activity (Charrier et al., 2015; Charrier and Anastasio, 2012), whereas others highlight the enhanced role of organics, in particular water soluble organic carbon (WSOC) such as HULIS, and quinones (Cho et al., 2005; Fang et al., 2016). Furthermore, several studies correlate volume-normalised OP measurements with compositional variability, but given the potential co-linearity of many aerosol components with overall mass, mass-normalised intrinsic OP values may provide additional insight into the effect of chemical composition on aerosol OP (Bates et al., 2019; Puthussery et al., 2020) (Bates et al., 2019; Puthussery et al., 2020). Thus, a comprehensive characterisation of gaseous and particle phase pollution conditions combined with measurements utilising multiple OP assays simultaneously, ~~providing~~provides a wide range of information on particle-bound ROS and aerosol OP, ~~would allow~~allowing the identification of the most important components that drive aerosol OP. Ultimately, a greater understanding of the specific aerosol characteristics that influence OP, as well as specific sources that contribute more to aerosol OP, could allow the development of more targeted and efficient air pollution mitigation

strategies. [Further details of the selection of OP assays, their scope and biological applicability are described in Section S2 of the Supplementary Information.](#)

In this work, PM<sub>2.5</sub> filter samples collected in winter 2016 and summer 2017 during the APHH campaign were analysed using four acellular methods; AA, DCFH, DTT and EPR, providing a wealth of [informationdata](#) on the health-relevant properties of PM<sub>2.5</sub> including particle-bound ROS, redox-active components contributing to aerosol OP, and the formation of superoxide radicals upon sample extraction. As the APHH campaign simultaneously captured [one of the most extensive and comprehensive datasets atmospheric composition datasets including](#) a broad range of PM compositional data, we aimed to establish what individual PM components, meteorological and atmospheric conditions contributed to increased OP assay response, whether these influences and compositions differed [substantially](#) between assays, and if the compositions reflected particular PM sources. We included 107 different measurements, comprising transition metals, AMS measurements, total elemental and organic carbon, and a broad panel of organic species relating to biomass and fossil fuel burning, cooking emissions, vehicular markers, secondary organic aerosol compounds, plus gaseous species and general atmospheric conditions. We ~~also~~ sought to investigate the differences between volume-based and mass-based responses, as mass-based analysis facilitates site and temporal comparisons more readily than volume measurements and provide details on intrinsic particle properties that influence OP. [In order to highlight underlying trends in such a broad and complex dataset, we also applied multivariate statistical analysis and developed multiple linear regression models to fully characterise the chemical compositional factors driving each assay response.](#)

## 2 Materials and methods

### 2.1 Air Pollution and Human Health in a Chinese Megacity Campaign (APHH)

#### 2.1.1 Site description

High-volume 24 hr aerosol filter samples were collected at the Institute of Atmospheric Physics (IAP) in Beijing, China (39°58'28" N, 116°22'15" E) (**Figure S1**). Winter PM was collected during the months of Nov-Dec 2016 and summer PM was collected during the months of May-June 2017.  $n = 31$  filters for winter 2016 and  $n = 34$  filters for summer 2017 were collected.

A PM<sub>2.5</sub> high-volume sampler (RE-6070VFC, TICSHE, USA) was used at a flow rate of  $\sim 1.06 \text{ m}^3/\text{min}$ . PM<sub>2.5</sub> for subsequent OP analysis was collected onto quartz microfiber filters (Whatman, 20.3 x 25.4 cm) with a collection area of 405 cm<sup>2</sup>.

#### 2.1.2 PM<sub>2.5</sub> composition, gas phase composition and meteorological data

Oxidative potential measurements were correlated with a range of additional particle phase composition, gas phase composition and meteorological measurements conducted concurrently during the APHH-Beijing campaign (Shi et al., 2019).

Briefly, the following composition data was collated: total organic and elemental carbon (OC, EC), soluble inorganic ions (K<sup>+</sup>,

Na<sup>+</sup>, Ca<sup>2+</sup>, NH<sub>4</sub><sup>+</sup>, NO<sub>3</sub><sup>-</sup>, SO<sub>4</sub><sup>2-</sup> and Cl<sup>-</sup>) measured using ion chromatography (IC), low-oxidised organic aerosol and more-oxidised organic aerosol (LOOOA/MOOOA) fractions using aerosol mass spectrometry (AMS), biomass burning markers (galactosan, mannosan and levoglucosan), 16 polycyclic aromatic hydrocarbons (PAHs) (see (Elzein et al., 2019, 2020)), C<sub>24</sub>-C<sub>34</sub> *n*-alkanes, aerosol cooking markers (palmitic acid, stearic acid, cholesterol), vehicle exhaust markers (17a(H)-22, 29,30-trisnorhopane (C27a) and 17b(H)-21a-norhopane (C30ba)), isoprene SOA markers (2-methylglyceric acid, 2-methylerythritol, 2-methylthreitol, 3-hydroxyglutaric acid), C<sub>5</sub>-alkene triols (cis-2-methyl-1,3,4-trihydroxy-1-butene, 3-methyl-2,3,4-trihydroxy-1-butene, trans-2-methyl-1,3,4-trihydroxy-1-butene),  $\alpha$ -pinene SOA tracers (cis-pinonic acid, pinic acid, 3-methyl-1,2,3-butanetricarboxylic acid (MBTCA), 2,3-dihydroxy-4-oxopentanoic acid, aged  $\alpha$ -pinene SOA marker),  $\beta$ -caryophyllene SOA tracer ( $\beta$ -caryophyllinic acid) and an aromatic volatile organic compound (VOC) SOA tracer (3-isopropylpentanedioic acid) (Liu et al., 2020). The following additional data was obtained from the Centre for Environmental Data Analysis (CEDA) archive:- concentrations of inorganic elements Al, Ti, V, Cr, Mn, Fe, Co, Ni, Cu, Zn, Cd, Sb, Ba and Pb in PM<sub>2.5</sub> using X-ray fluorescence (XRF) (Xu et al., 2020a), gas phase concentrations of methanol, acetonitrile, acetaldehyde, acrolein, acetone, isoprene, methacrolein, methyl ethyl ketone, benzene, toluene, C<sub>2</sub>-benzenes and C<sub>3</sub>-benzenes measured using proton transfer reaction time-of-flight mass spectrometry (PTR-ToF-MS) (Acton et al., 2018), gas phase concentrations of O<sub>3</sub>, CO, NO, NO<sub>2</sub>, NO<sub>y</sub> and SO<sub>2</sub> as well as relative humidity (RH) and air temperature measurements (Shi et al., 2019), photolysis rates for J O<sup>1</sup>D and J NO<sub>2</sub> (Whalley et al., 2020) and gas phase concentrations of hydroxyl radicals (OH), peroxy radicals (HO<sub>2</sub>) and organic peroxy radicals (RO<sub>2</sub>) measured using fluorescence assay gas expansion (FAGE) (Whalley et al., 2020).

## 2.2 Oxidative potential measurements

### 2.2.1 Reagents

Chemicals and gases were obtained from Sigma-Aldrich unless otherwise indicated and were used without further purification: ascorbic acid ( $\geq 99.0$  %), Chelex<sup>TM</sup> 100 sodium form, 0.1 M HCl solution, 0.1 M NaOH solution, dichlorofluorescein-diacetate (DCFH-DA), 1 M potassium phosphate buffer solution, horseradish peroxidase (HRP), methanol (HPLC grade), and *o*-phenylenediamine ( $\geq 99.5$  %). H<sub>2</sub>O used for the DCFH, HRP and AA solution were obtained from a Milli-Q high purity water unit (resistivity  $\geq 18.2$  M  $\Omega$  cm<sup>-1</sup>, Merck Millipore, USA). For DTT analysis, 9,10-phenanthrenequinone (PQN) ( $\geq 99$  %), 5,5'-dithiobis(2-nitrobenzoic acid) (DTNB) (99 %), DL-dithiothreitol (DTT) ( $\geq 98$  %), potassium phosphate dibasic ( $\geq 98$  %, Krebs buffer), potassium phosphate monobasic ( $\geq 98$  %, Krebs buffer), and methanol ( $\geq 99.9$  %) were all obtained from Fisher Chemical. Nitrogen (oxygen free) was obtained from BOC (Cambridge, UK).

### 2.2.2 Acellular oxidative potential assays

Four offline acellular methods for measuring PM<sub>2.5</sub> oxidative potential and particle-bound ROS were utilised in this work; The DCFH/HRP assay (Fuller et al., 2014), which quantifies the fluorescent product 2,7-dichlorofluorescein, the ascorbic acid

(AA) assay (Campbell et al., 2019) an assay that is particularly sensitive to species which are likely particle-bound ROS, the ascorbic acid (AA) assay (Campbell et al., 2019) which quantifies the dominant product of AA oxidation, dehydroascorbic acid (DHA) via condensation with a dye and fluorescence spectroscopy. This is an AA-only assay and does not contain other components normally present in synthetic lung fluid (SLF); filter extracts are performed at pH 7, whereas the AA reaction with the filter extract is performed at pH 2 to improve assay stability and sensitivity (Campbell et al., 2019). Electron Paramagnetic Resonance spectroscopy (EPR) (Miller et al., 2009) specifically ~~for~~targets the measurement of superoxide ( $O_2^{\cdot-}$ ) and the dithiothreitol (DTT) assay (e.g. Cho et al., 2005), which quantifies the rate of loss of DTT via absorbance measurements. These acellular methods have been widely applied in the literature to study particle OP (Bates et al., 2019) and particle-bound ROS (Bates et al., 2019). For detailed descriptions of the assay protocols, see Section S2 in the supplementary information S3 in the Supplementary Information. Assessing OP and particle-bound ROS in filters with the aforementioned assays is ~~done~~performed offline. There is potential to underestimate PM OP and particle-bound ROS using offline filter-based analysis, as short-lived components which contribute to particle-bound ROS and OP may undergo degradation prior to analysis. However, using an offline method allows the opportunity to correlate with a wide range of additional composition measurements, allowing a more explicit characterisation of the chemical components of PM that contribute to observed acellular assay responses.

Formatted: Font: Italic

### 2.3 Statistical analysis

We aimed to analyse the data as thoroughly as possible with respect to characterising the OP measured by each assay, and to attempt to robustly connect assays to both individual measurements and potential PM sources. As data were collated from several different experimental projects, and as analytical uncertainty values were not available for the majority of the data, the use of positive matrix ~~factorization~~factorisation (PMF) was not undertaken for source apportionment, and will be published subsequently for selected analyses (Xu et al., 2020a)(Xu et al., 2020a). Multiple analytical platforms were used for the acquisition of compositional data, uncertainty estimates for each measurement were not easily estimable, a factor-based chemical mass balance approach was not required specifically, and temperature, relative humidity, actinic flux and other non-mass measurements could also be influential on the OP response, and are factors mainly independent of PM sources. On this basis we considered that PMF would not ultimately give useful models in the ~~OP~~specific context of OP. However, these issues are managed adequately by principal components analysis (PCA), which is a useful general unsupervised method for examining underlying variance and latent effects in data, and handles multicollinearity well, although it is not optimal for chemical mass balance source apportionment (Paatero and Tapper, 1994).

PCA and partial least squares regression (PLSR) models were produced in SIMCA+ 16.0 (Umetrics, Umeå, Sweden). Missing values were not altered prior to model construction, although measurements with more than 56% missing values per season were discarded from models.  $R^2$  and  $Q^2$  values were used to assess the goodness-of-fit of the model and the goodness-of-prediction of the data through 7-fold cross-validation respectively. Data were unit-variance scaled and mean-centred to remove

effects related to absolute data magnitude. Models were allowed to optimise to the maximum number of latent variables (LV) at which the cumulative  $Q^2$  value stabilised, which for most PLSR models was a single LV. PLSR model robustness was assessed through permutation testing, where the classifier (i.e. OP assay response) for all samples was randomly permuted 999 times and the PLSR model constructed for each permutation; the model was considered robust if the real model  $R^2$  and  $Q^2$  values outperformed those from all random permutation models. Negative  $Q^2$  values indicate no predictive power of the data in the model, and LVs with  $Q^2$  significantly lower than the  $R^2$  value (arbitrarily defined for this study as  $Q^2$  at more than 10% below the  $R^2$ ) can be considered at least partially overfitted.

Spearman rank correlations ( $R_s$ ) between OP measurements and  $PM_{2.5}$  were calculated using OriginPro (2020) or R, and were used to assess the relationships between assay responses and individual measurements, with Mann-Whitney-U tests (in R) used for pairwise testing of the differences in seasonal response for both assays and individual measurements. All other multivariate analyses, multiple linear regression models and selected univariate analyses were produced in R 4.0.2 (R Core Team, Vienna, Austria), implemented in RStudio 1.3.959 (Boston, Massachusetts, USA).

For multiple linear regression models, outlier values were arbitrarily deemed to be those greater than 5 times the standard deviation and replaced with the season median where appropriate for analysis. Measurement subsets manually selected as relevant to source composition were then subjected to a variable selection process, whereby pairwise Spearman correlations for all measurements were calculated, and measurements removed from subsets if they were highly correlated with other measurements but predicted OP more poorly than the other co-correlated measurements, to reduce the number of variables contributing identical information in the final models. Multiple linear regression models were then further optimised from this initial subset using the *regsubsets* function in the *leaps* R package, to allow for between 4-8 variables which best predicted the OP response (models could be constructed with fewer or even more measurements, but the aim was to examine a small panel of contributors to potential source compositions). The variable selection process precludes the use of linear regression mode performance indicators such as the Aikake or Bayesian information criteria, as the model component sets are not identical.

The stability of model predictions and features were assessed using bootstrap resampling of data, by randomly splitting one fifth of the data as a test set and using the remaining samples to construct the model and predict the left-out samples, for 500 random iterations. Stability was also assessed through overall variance in OP predictions, measurement feature coefficients and model residuals plots, and run order/date bias (not differentiable as samples were analysed in date order) was assessed in residuals plots. Although not all data distributions were strictly normal when examined in the univariate kernel density plots, data were not log-transformed for multiple linear regression models, as this creates non-linearity in the model component response, which can complicate interpretation. Model residuals were plotted for manual examination and were all generally normally distributed despite the relatively small number of samples, and biases were related to periods of missing measurements or samples with values below the limit of quantification. Code developed for analysis is publicly available at <https://github.com/katewolfer/Beijing>.



260 3 Results and discussion

Both volume-normalised ( $OP_v$ , per  $m^3$  air) and particle mass normalised ( $OP_m$ , per  $\mu g PM_{2.5}$ ) values are considered in this work, where the  $OP$  value of the specific assay and sample is normalised by the volume of air collected or by the total  $PM_{2.5}$  mass on the filter, respectively.  $OP_v$  is useful when considering exposure or epidemiological outcomes, but  $OP_m$  is likely a more informative metric when exploring how chemical composition influences  $PM_{2.5}$   $OP$ , and potentially enabling better  $OP$  response, site and composition intercomparisons (Bates et al., 2019)(Bates et al., 2019). Henceforth, assay- $OP$ -values $OP_v$  and  $OP_m$  will be used when discussing the overall response of all four methods; specific discussion of the acellular methods will be referred to as  $AA_v$ ,  $DTT_v$ ,  $DCFH_v$  and  $EPR_v$  for volume-normalised  $OP_v$ -values, and  $AA_m$ ,  $DTT_m$ ,  $DCFH_m$  and  $EPR_m$  for mass-normalised  $OP_m$ -values. For comparison of mass normalised  $OP_m$  values,  $PM_{2.5}$  composition measurements were also normalised for total PM mass (*e.g.* ng/ $\mu g$  per  $\mu g PM_{2.5}$ )

Formatted: Subscript

Formatted: Font: Italic

270 3.1 Seasonal variation of  $OP_m$  and  $OP_v$

24-hour  $PM_{2.5}$  mass concentrations in winter 2016 (08/11/2016-09/12/2016) ranged from  $8.1 - 328.7 \mu g m^{-3}$ , with an average  $PM_{2.5}$  mass of  $98.7 \pm 75 \mu g m^{-3}$ , whereas in summer 2017 (21/05/2017-24/06/2017)  $PM_{2.5}$  concentrations ranged of  $13.6 - 85 \mu g m^{-3}$  with an average of  $36.7 \pm 16 \mu g m^{-3}$  (Figure S7) (Shi et al., 2019; Xu et al., 2020a). Average seasonal values for each assay are summarised in Table S1. AAn example data set showing 24-hr average data, for  $AA_v$  and  $PM_{2.5}$  mass in both the winter and summer campaign, is shown in Figure 1 (for  $DCFH_v$ ,  $DTT_v$  and  $EPR_v$ , see Section S5S6 “Summary statistics for all measurements” in the Supplementary Information).

Formatted: Font: Bold

Formatted: Font: Bold

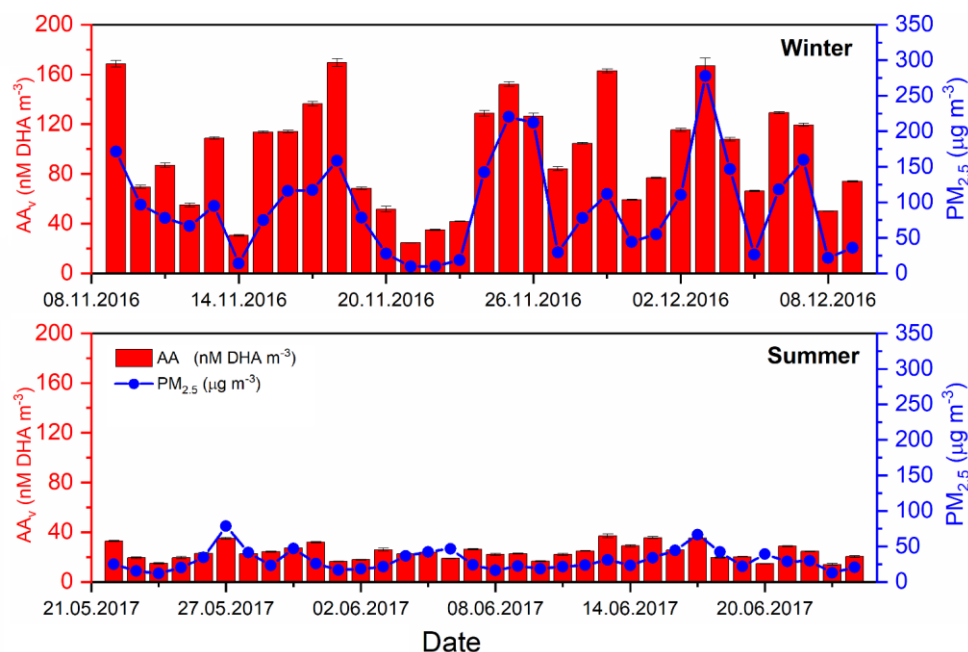


**Figure 1.** 24-hour averaged volume-normalised AA<sub>v</sub> (red bars) and PM<sub>2.5</sub> mass (blue dots), analysed from 24-hour high volume filters, for both winter 2016 (08/11/2016 – 08/12/2016) and summer 2017 (21/05/2017 – 24/06/2017) (Shi et al., 2019; Xu et al., 2020a). Substantially higher average PM<sub>2.5</sub> mass concentrations (μg m<sup>-3</sup>) and AA<sub>v</sub> were observed in the winter season compared to the summer (see Table S1 for summary). [DCFH<sub>v</sub>, DTT<sub>v</sub> and EPR<sub>v</sub> 24-hour averaged datasets can be found in Figures S8-S10 respectively.](#)

For all assays, a higher average PM<sub>2.5</sub> OP<sub>v</sub> was observed in the winter compared to the summer in Beijing (**Table S1**). The average AA<sub>v</sub> was  $96.7 \pm 42.7$  nM [DHA] m<sup>-3</sup> in the winter, whereas a mean value of  $24.1 \pm 6.1$  nM [DHA] m<sup>-3</sup> was observed in the summer. Given the recent introduction of this AA-based assay, which measures the formation of the AA oxidation product DHA rather than measuring the decay of AA *via* UV absorbance, limited literature values are available for direct comparison (Campbell et al., 2019b; Campbell et al., 2019a). Average DCFH<sub>v</sub> in the winter was  $0.71 \pm 0.52$  nmol H<sub>2</sub>O<sub>2</sub> m<sup>-3</sup> compared to  $0.17 \pm 0.11$  nmol H<sub>2</sub>O<sub>2</sub> m<sup>-3</sup> in the summer, which is within the range of DCFH<sub>v</sub> values observed in previous studies in Taiwan, the USA and Singapore (OP<sub>DCFH</sub> 0.02 – 5.7 nmol H<sub>2</sub>O<sub>2</sub> m<sup>-3</sup>) (Hasson and Paulson, 2003; Hewitt and Kok, 1991; Hung and Wang, 2001; See et al., 2007; Venkatachari et al., 2005). Mean observed values for DTT<sub>v</sub> in the winter and summer were  $2.9 \pm 0.11$  nmol min<sup>-1</sup> m<sup>-3</sup> and  $0.9 \pm 0.40$  nmol min<sup>-1</sup> m<sup>-3</sup>, respectively. The mean values of DTT<sub>v</sub> observed in this study are greater than those measured in similar studies in Beijing (Liu et al., 2014) (0.11–0.49, mean = 0.19 nmol min<sup>-1</sup> m<sup>-3</sup>) with similar mass concentrations of PM<sub>2.5</sub> (mean = 140 μg m<sup>-3</sup>), although they are within the range of DTT<sub>v</sub> values

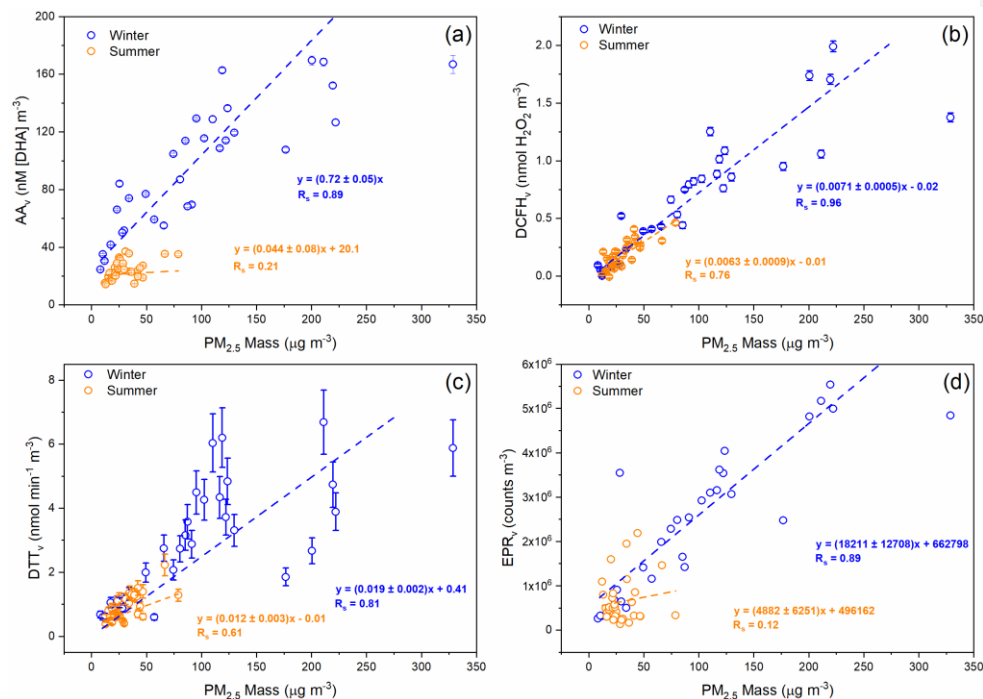
observed in a number of previous studies in several locations, including Europe (Jedynska et al., 2017; Yang et al., 2015), the  
295 US (Fang et al., 2015; Verma et al., 2014) and Northern China (Liu et al., 2018) ( $0.1\text{--}14.7\text{ nmol min}^{-1}\text{ m}^{-3}$ ). The mean  $\text{EPR}_v$   
values, relating to the specific detection of  $\text{O}_2^{\cdot-}$ , were  $2.4 \times 10^6 \pm 1.6 \times 10^6$  and  $5.8 \times 10^5 \pm 4.1 \times 10^6$  counts  $\text{m}^{-3}$  in the winter and  
summer campaign, respectively.

Spearman rank correlation coefficients ( $R_s$ ) of aerosol  $\text{OP}_v$  with  $\text{PM}_{2.5}$  vary between the winter and summer season, and also  
between OP assays, as illustrated in **Figure 2**. All four assays, when normalised per volume ( $\text{OP}_v$ ), show a stronger  
300 correlation with  $\text{PM}_{2.5}$  mass concentration in the winter compared to the summer, consistent with results observed in Chamonix,  
France by Calas *et al.* (Calas *et al.*, 2018). For example,  $\text{DCFH}_v$  correlates well with 24-hr average total  $\text{PM}_{2.5}$  mass  
concentration ( $\mu\text{g m}^{-3}$ ) in both winter ( $R_s = 0.96$ ) and summer ( $R_s = 0.76$ ). All four assays, when normalised per volume  
( $\text{OP}_v$ ), show a stronger correlation with  $\text{PM}_{2.5}$  mass concentration in the winter compared to the summer, consistent with results  
305 observed in Chamonix, France by Calas *et al.* (Calas *et al.*, 2018). For example,  $\text{DCFH}_v$  correlates well with 24-hr average total  
 $\text{PM}_{2.5}$  mass concentration ( $\mu\text{g m}^{-3}$ ) in both winter ( $R_s = 0.96$ ) and summer ( $R_s = 0.76$ ) (**Figure 2B**), whereas  $\text{AA}_v$   
correlates well in the winter ( $R_s = 0.89$ ) and poorly in summer ( $R_s = 0.21$ ). Similar correlations of  $\text{DCFH}_v$  with  $\text{PM}_{2.5}$  mass  
concentrations in both winter and summer suggest that species influencing  $\text{DCFH}_v$  variability (e.g.  $\text{H}_2\text{O}_2$  and organic peroxides,  
likely particle-bound ROS) present in the particles are relatively consistent between both seasons. Similar to  $\text{AA}_v$ , differences  
between the seasons are also observed for  $\text{DTT}_v$  and  $\text{EPR}_v$ , where correlations of aerosol  $\text{OP}_v$  vs.  $\text{PM}_{2.5}$  are stronger in winter  
310 compared to summer (**Figure 2C and 2D**), also generally consistent with previous studies, although in contrast to  
Calas *et al.* (2018), who observed no difference in  $\text{EPR}_v$  between seasons in Chamonix, although in that study the spin-trap  
 $\text{DMPO}$  was used to study hydroxyl radicals, whereas in this study we focus on the formation of superoxide upon particle  
suspension in aqueous solution. The differences in the correlation shown in **Figure 2** suggests that the four assays are sensitive  
to different PM components and that in winter and summer different PM sources or components are important for the assay's  
315 responses (Calas *et al.*, 2018; Saffari *et al.*, 2013; Verma *et al.*, 2014). **Figure 2** demonstrates that  $\text{PM}_{2.5}$  mass could be a  
reasonable predictor of total  $\text{OP}_v$  in winter but the poorer correlations between all  $\text{OP}_v$  assays and  $\text{PM}_{2.5}$  in the summer indicate  
that a more detailed understanding is necessary to elucidate and ultimately predict aerosol OP. However, the variability in the  
strength of correlation between  $\text{OP}_v$  and  $\text{PM}_{2.5}$  mass as well as the seasonal difference indicates that compositional differences  
in  $\text{PM}_{2.5}$  or additional atmospheric processes influence  $\text{PM}_{2.5}$  OP.

Formatted: Font: Bold

Formatted: Font: Bold

Formatted: Font: Bold



**C and 2D)**, also generally consistent with previous studies, although in contrast to Calas et al. (2018), who observed no difference in  $EPR_v$  between seasons in Chamonix, although in that study the spin trap DMPO was used to study hydroxyl radicals, whereas in this study we focus on the formation of superoxide upon particle suspension in aqueous solution. The differences in the correlation shown in **Figure 2** suggests that the four assays are sensitive to different PM components and that in winter and summer different PM sources or components are important for the assay's responses (Calas et al., 2018; Saffari et al., 2013; Verma et al., 2014). **Figure 2** demonstrates that  $PM_{2.5}$  mass could be a reasonable predictor of total  $OP_v$  in winter but the poorer correlations between all  $OP_v$  assays and  $PM_{2.5}$  in the summer indicate that a more detailed understanding is necessary to elucidate and ultimately predict aerosol OP. However, the variability in the strength of correlation between  $OP_v$  and  $PM_{2.5}$  mass as well as the seasonal difference indicates that compositional differences in  $PM_{2.5}$  or additional atmospheric processes influence  $PM_{2.5}$  OP.

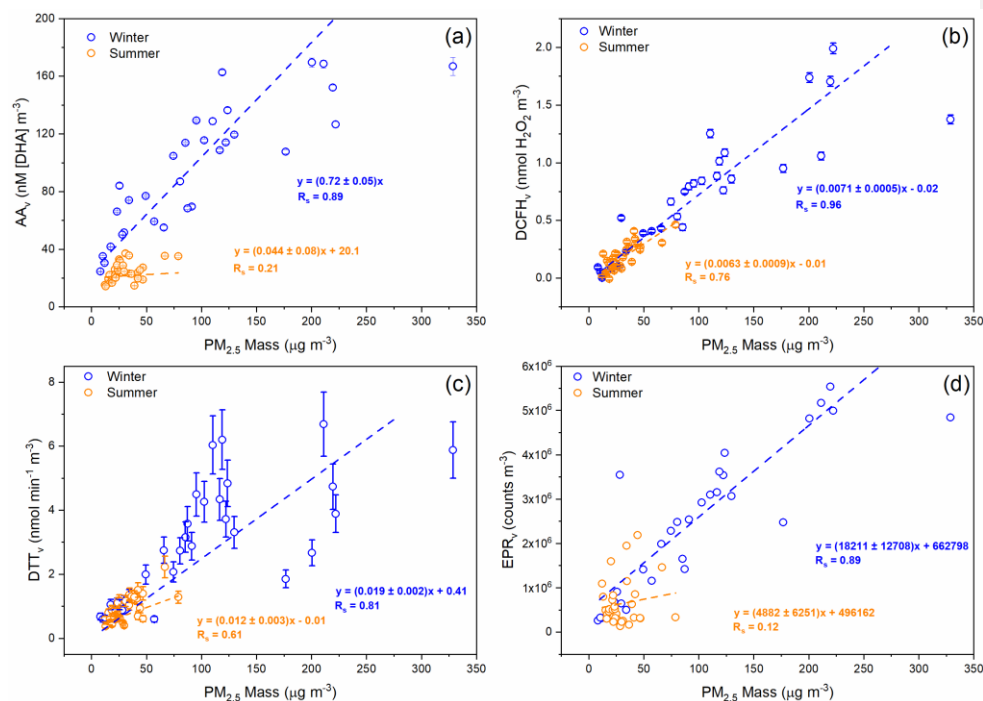
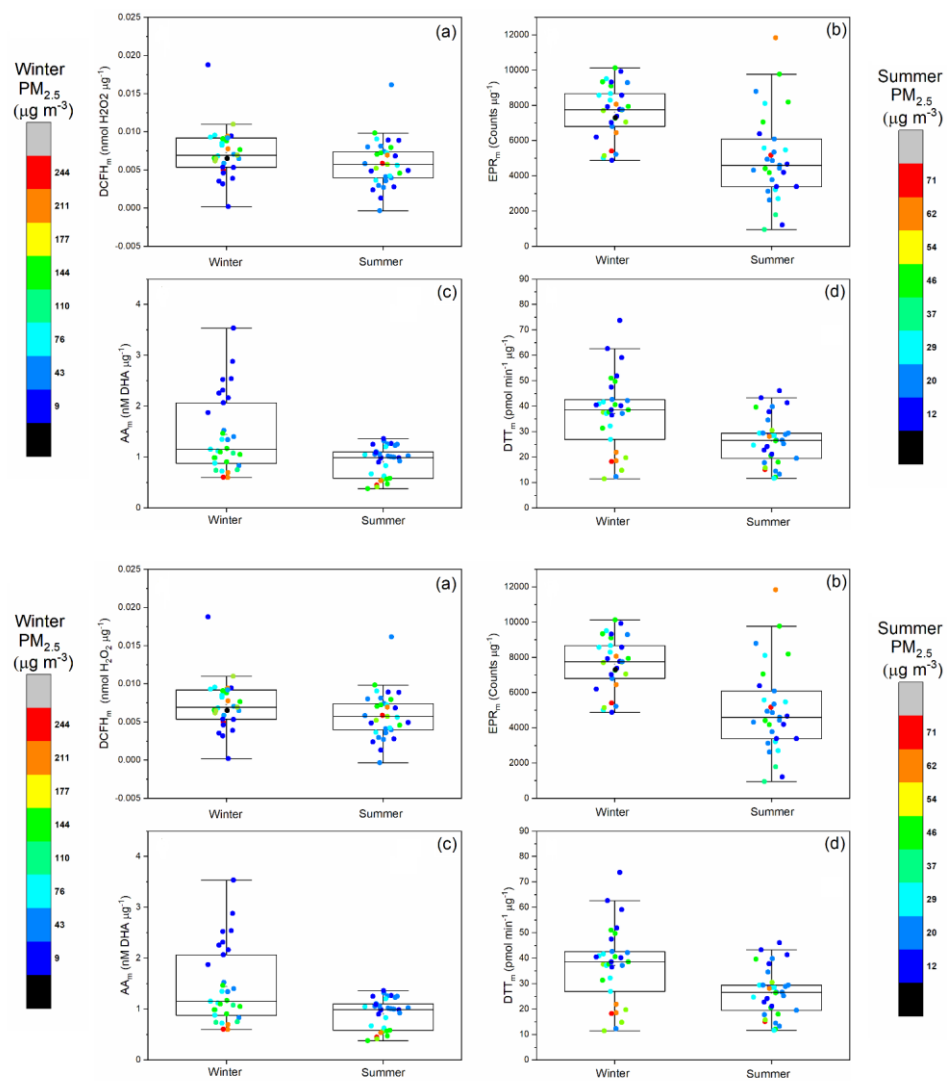


**Figure 2.** Comparison of PM<sub>2.5</sub> OP<sub>v</sub> during winter 2016 (blue) and summer 2017 (orange) vs. PM<sub>2.5</sub> mass (μg m<sup>-3</sup>). (a) AA<sub>v</sub>, (b) DCFH<sub>v</sub>, (c) DTT<sub>v</sub>, and (d) EPR<sub>v</sub>. Each datapoint represents a 24-hour average for OP measurements and PM<sub>2.5</sub> mass. Corresponding R<sub>s</sub> and linear fit equations are included. For AA<sub>v</sub>, DCFH<sub>v</sub>, and DTT<sub>v</sub>, error bars represent the standard deviation observed over three repeat measurements for each filter sample, and in some cases the error is smaller than the data point. Uncertainty values are unavailable for EPR<sub>v</sub> measurements.

To gain further insights into the potential particle-level compositional differences underlying assay OP response, the OP data for the four assays was normalised to the PM<sub>2.5</sub> mass in each sample. As shown in **Figure 3**, mass-normalised OP<sub>m</sub> values vary up to a factor of ten within a single season. AA<sub>m</sub>, DCFH<sub>m</sub>, DTT<sub>m</sub> and EPR<sub>m</sub> for both winter and summer are [also](#) displayed in **Figure 3**, with colour bars indicating the 24-hr average total PM<sub>2.5</sub> mass (μg m<sup>-3</sup>) for the corresponding OP<sub>m</sub> measurement. The average OP<sub>m</sub> response observed in this study shows a similar trend to OP<sub>v</sub> (**Table S2**), where higher OP<sub>m</sub> values are observed for winter compared to summer (**Figure 3**), as observed previously (Liu et al., 2018; Saffari et al., 2014). This demonstrates that there are specific properties of PM<sub>2.5</sub> in the winter that result in overall higher intrinsic OP<sub>m</sub> compared to the summer.

For  $AA_m$ , an inverse relationship between total  $PM_{2.5}$  mass concentration and  $AA_m$  is observed in both seasons, where days with high  $PM_{2.5}$  mass loadings have correspondingly low  $AA_m$  values in both the winter and summer, with almost a factor of 6 difference between the  $AA_m$  on the highest  $PM_{2.5}$  mass day ( $PM_{2.5} = 328 \mu g m^{-3}$ ,  $AA_m = 0.6 nM [DHA] \mu g^{-1}$ ) and lowest  $PM_{2.5}$  mass day observed during the winter campaign ( $PM_{2.5} = 8 \mu g m^{-3}$ ,  $AA_m = 3.53 nM [DHA] \mu g^{-1}$ ). A similar trend is observed for  $DTT_m$ , where in general days with higher overall  $PM_{2.5}$  mass concentrations have correspondingly low  $DTT_m$  values, which has also been observed previously (Wang et al., 2020b). The  $DTT_m$  response is also not correlated with Cu and Mn concentrations, despite the non-linear but monotonic relationship between these components being demonstrated in other studies (Charrier et al., 2016)(Charrier et al., 2016). These results indicate that on high-pollution days a large fraction of the PM mass might be OP-inactive, resulting in low intrinsic  $OP_m$  values. In general, smaller particles have been observed to have higher  $DTT_m$  values compared to larger particles (Bates et al., 2019; Janssen et al., 2014)(Bates et al., 2019; Janssen et al., 2014), an effect which may also play a role here. Another possibility is that on higher  $PM_{2.5}$  mass days, selected chemical species interact with or deactivate redox-active components present in  $PM_{2.5}$  (e.g. interaction of organics with metals (Tapparo et al., 2020), therefore reducing the observed  $OP_m$  signal. It is also possible that components present in  $PM_{2.5}$  on higher  $PM_{2.5}$  mass concentration days interfere with the assay response. It is currently unclear which chemical components are responsible for the observed inverse relationship between  $PM_{2.5}$  mass with  $AA_m$  and  $DTT_m$ . However, statistically significant inverse correlations are observed between  $AA_m$  and  $DTT_m$  in both the winter and summer with the chemically undetermined “unknown” fraction of  $PM_{2.5}$  for  $DTT_m$  ( $R_s = -0.81$ ) and  $AA_m$  ( $R_s = -0.75$ ), implying that  $PM_{2.5}$  chemical components unaccounted for in this study are likely responsible for the lower intrinsic  $AA_m$  and  $DTT_m$  values on high  $PM_{2.5}$  mass days (See Section 3.2 “Univariate analysis of PM OP and additional measurements”, Figure S11 and Figure S12).

In contrast, higher  $DCFH_m$  responses are observed on days with greater  $PM_{2.5}$  mass concentrations in both winter and summer. Increased  $DCFH_m$  responses on more polluted days could indicate that the mass fraction of particle-bound ROS (e.g. organic peroxides from SOA) increases with increasing  $PM_{2.5}$  mass concentration, or that the capacity of PM components to produce  $H_2O_2$  upon extraction, as measured by  $DCFH$ , is enhanced. ~~Previous studies have shown that on a mass normalised basis, larger particles ( $PM_{4.0}$ ) have greater potential for  $H_2O_2$  generation in synthetic lung fluid, possibly via Fenton type chemistry, as compared to smaller particles ( $PM_{2.5}$ ) (Shen et al., 2011; Shen and Anastasio, 2011), likely related to components in smaller particles that relate to their specific sources. Despite the significant seasonal difference in  $EPR_m$ , no obvious relationship between  $EPR_m$  and  $PM_{2.5}$  mass was observed in our study.~~ Despite the significant seasonal difference in  $EPR_m$ , no obvious relationship between  $EPR_m$  and  $PM_{2.5}$  mass was observed in our study. There is potential to underestimate PM OP and particle-bound ROS using offline filter-based analysis, as short-lived components which contribute to particle-bound ROS and OP may undergo degradation prior to analysis. However, using an offline based method allows the opportunity to correlate with a wide range of additional composition measurements, allowing a more explicit characterisation of the chemical components of PM that contribute to observed acellular assay responses.



380 **Figure 3.** Summer and winter 24-hour averaged mass-normalised OP<sub>m</sub> (**Aa**) AA<sub>m</sub> (μM DHA μg<sup>-1</sup>), (**Bb**) DCFH<sub>m</sub> (nmol H<sub>2</sub>O<sub>2</sub> μg<sup>-1</sup>), (**Cc**) EPR<sub>m</sub> (counts μg<sup>-1</sup>) and (**Dd**) DTT<sub>m</sub>. Box plots indicate the median, 25% and 75% percentiles, and the data range. Data points are colour coded with respect to the 24-hour average PM<sub>2.5</sub> mass (μg m<sup>-3</sup>), with a separate colour scale for winter and summer PM<sub>2.5</sub> masses given the difference in total PM<sub>2.5</sub> masses observed between the seasons.

Spearman rank correlations (R<sub>s</sub>) between the four assays, for mass-normalised OP<sub>m</sub> and volume-normalised OP<sub>v</sub> are presented in **Table 1**~~Table 1~~. In terms of OP<sub>v</sub>, all four assays show significantly strong correlations with each other in the winter season (R<sub>s</sub> 0.72 – 0.89), but weaker correlations are observed between assays in the summer (R<sub>s</sub> 0.01-0.58), a seasonal difference observed previously by Calas et al. (~~2018~~[\(2018\)](#)). In contrast, the only statistically significant correlation observed for OP<sub>m</sub> is between AA<sub>m</sub> and DTT<sub>m</sub> in the winter season only (R<sub>s</sub> = 0.58).

Seasonality of both OP<sub>v</sub> and OP<sub>m</sub> observed in the assays could be driven by changes in PM sources influencing overall OP, or a number of physical and chemical factors directly affecting particle composition. For instance, lower ambient temperatures in the winter may increase the partitioning of semi-volatile organic compounds, such as ~~quinones~~small [quinones \(e.g. anthracenequinone and 2,3-dimethylanthraquinone \(Delgado-Saborit et al., 2013\)\)](#) and nitro-PAHs, which have been shown to influence DTT activity (Ntziachristos et al., 2007; Verma et al., 2011), observations which are supported by lab-based studies showing decreasing aerosol OP at higher temperatures (Biswas et al., 2009; Verma et al., 2011). Changing boundary layer height between the seasons may also contribute to higher concentrations of species [which correlate with PM<sub>2.5</sub> mass](#) responsible for increasing aerosol OP during the winter, compared to summer, especially affecting OP<sub>v</sub> seasonality (Wang et al., 2020a). Furthermore, air mass history may play an important role in the observed seasonality of OP. For instance, it was observed that winter days with high PM<sub>2.5</sub> mass concentrations typically originate from regional sources south of Beijing, which is widely industrialised, whereas high mass days in the summer typically have more varied air mass histories (Panagi et al., 2020; Steimer et al., 2020). There are likely varying contributions between different sources in different seasons, e.g. more photochemistry in the summer driving oxidation and biogenic sources, and more contributions from residential heating combustion in the winter (Xu et al., 2020a). In order to gain further insight into what causes the observed variability of OP, relationships between particle chemical composition and aerosol OP will be explored in detail below.

405 **Table 1.** Correlation of volume-normalised (OP<sub>v</sub>, top panel) and mass-normalised (OP<sub>m</sub>, bottom panel) assay responses in the winter (blue) and summer (orange) campaign. It should be noted that assay responses expressed as mass-normalised (OP per μg) are correlated with mass-normalised additional particle phase composition measurements (i.e. μg or ng per μg PM<sub>2.5</sub>).

OP <sub>v</sub> R <sub>s</sub>	AA <sub>v</sub>	DCFH <sub>v</sub>	EPR <sub>v</sub>	DTT <sub>v</sub>
AA <sub>v</sub>		0.89***	0.86***	0.83***
DCFH <sub>v</sub>	0.35*		0.86***	0.72***
EPR <sub>v</sub>	0.19	0.01		0.88***
DTT <sub>v</sub>	0.41*	0.58***	0.07	

Formatted: Font: Bold



<b>OP<sub>m</sub> R<sub>s</sub></b>	<b>AA<sub>m</sub></b>	<b>DCFH<sub>m</sub></b>	<b>EPR<sub>m</sub></b>	<b>DTT<sub>m</sub></b>
<b>AA<sub>m</sub></b>		-0.29	0.22	<b>0.60**</b>
<b>DCFH<sub>m</sub></b>	-0.20		-0.08	-0.15
<b>EPR<sub>m</sub></b>	-0.26	0.15		0.27
<b>DTT<sub>m</sub></b>	0.2	-0.28	0.14	

Bold indicates  $R_s \geq 0.5$ , \* $p < 0.05$ , \*\* $p < 0.01$ , \*\*\*  $p < 0.001$ .

### 3.2 Univariate analysis of PM OP<sub>m</sub> and additional measurements

Spearman rank correlations between OP<sub>m</sub> of the four assays and 107 additional measurements conducted during the APHH campaign (see **Section 2.1.2** “PM<sub>2.5</sub> composition, gas phase composition and meteorological data”), were calculated for both the winter ( $n = 31$ ) and summer ( $n = 33$ ). We focus on OP<sub>m</sub> in the forthcoming discussion; as mentioned previously, as we consider it a particularly informative metric when determining the role of chemical composition on OP ([Bates et al., 2019](#); [Puthussery et al., 2020](#)) (all results are presented in **Section S7** “Assay correlations with individual component measurements”). ([Bates et al., 2019](#); [Puthussery et al., 2020](#)) (all univariate statistical summaries are presented in **Section S8**). The majority of additional particle phase composition, gas phase composition and meteorological measurements differed significantly by season. Exceptions included Al, V, Zn, Pb, Ca<sup>2+</sup>, Na<sup>+</sup>, NH<sub>4</sub><sup>+</sup>, acetaldehyde, acetonitrile, methanol, methyl ethyl ketone, methyl vinyl ketone/methacrolein, trans-2-methyl-1,3,4-trihydroxy-1-butene, β-caryophyllinic acid, 3-hydroxyglutaric acid, C5-alkene triols, cholesterol, LOOOA and MOOOA. Stacked bar plots illustrating the total daily concentrations for both mass-normalizednormalised and volume-normalizednormalised data are shown in **Figure 4** and **Figure S13**. Total concentrations of individual PM components (excluding all composite measures) account for approximately 0.3-0.8 μg/μg, i.e. 30 – 80% of the total PM mass (data not shown). Interestingly there were no marked or characteristic changes in mass composition associated with haze days; however, haze events were generally correlated with increased biomass burning marker concentration and total organic carbon in winter for the mass-normalised data (also observed during recent later winter haze events in Beijing ([Li et al., 2019](#))), and small inorganic ion concentrations in both seasons in the volume-normalised data (**Figure S13**).

IC measurements (K<sup>+</sup>, Na<sup>+</sup>, Ca<sup>2+</sup>, NH<sub>4</sub><sup>+</sup> NO<sub>3</sub><sup>-</sup> and SO<sub>4</sub><sup>2-</sup>) account for the greatest proportion of total particle mass in both seasons, all of which are major components of secondary inorganic PM mass (NH<sub>4</sub><sup>+</sup>, NO<sub>3</sub><sup>-</sup>, SO<sub>4</sub><sup>2-</sup>), mineral dust (Ca<sup>2+</sup>, K<sup>+</sup>), and marine aerosols (Na<sup>+</sup>, Cl<sup>-</sup>). These species were present at higher daily concentrations in summer than in winter. Summer compositions for each category were generally consistent for the whole sampling period, with a larger total proportion of SOA markers, whereas winter compositions were more variable, with greater contributions from elemental carbon, PAHs, *n*-alkanes and cooking-related compounds than for summer samples. Although PAHs are not redox-active ([Charrier and Anastasio, 2012](#))([Charrier and Anastasio, 2012](#)), they are precursors to redox-active oxy-PAHs (quinones) and nitro-PAHs ([Atkinson and](#)

Formatted: Font: Not Bold

435 Arey, 2007), and have well-established intrinsic cellular toxicity (reviewed in Moorthy et al., 2015), mediated by their  
conversion to hydroxy-PAHs, which exert mutagenic and teratogenic effects, and also inducing transcriptional modifications  
and oxidative stress. EC and *n*-alkanes are also non-redox-active and the exact mechanism of their toxicities is unclear (Levy  
et al., 2012); however, SOA derived from the interaction of *n*-alkanes with NO<sub>x</sub> with photo-oxidation (Lim and Ziemann,  
2005; Presto et al., 2010) is likely both to contribute to the redox activity of samples (Tuet et al., 2017), and to have more toxic  
440 properties than its precursors (Xu et al., 2020b). The sample from 22 November 2016 has a particularly high concentration of  
cooking markers (palmitic acid, stearic acid and cholesterol). This could reflect the fact that the traditional Chinese winter  
solar term Xiao Xue (小雪, “Light Snow”), begins on this date (Li, 2006), a period associated with the preparation of warm  
foods as the ambient temperatures in northern China drop; a similar elevation of palmitic acid and stearic acid has been  
observed around the same week in a more recent study in Shanghai (Wang et al., 2020c).

445

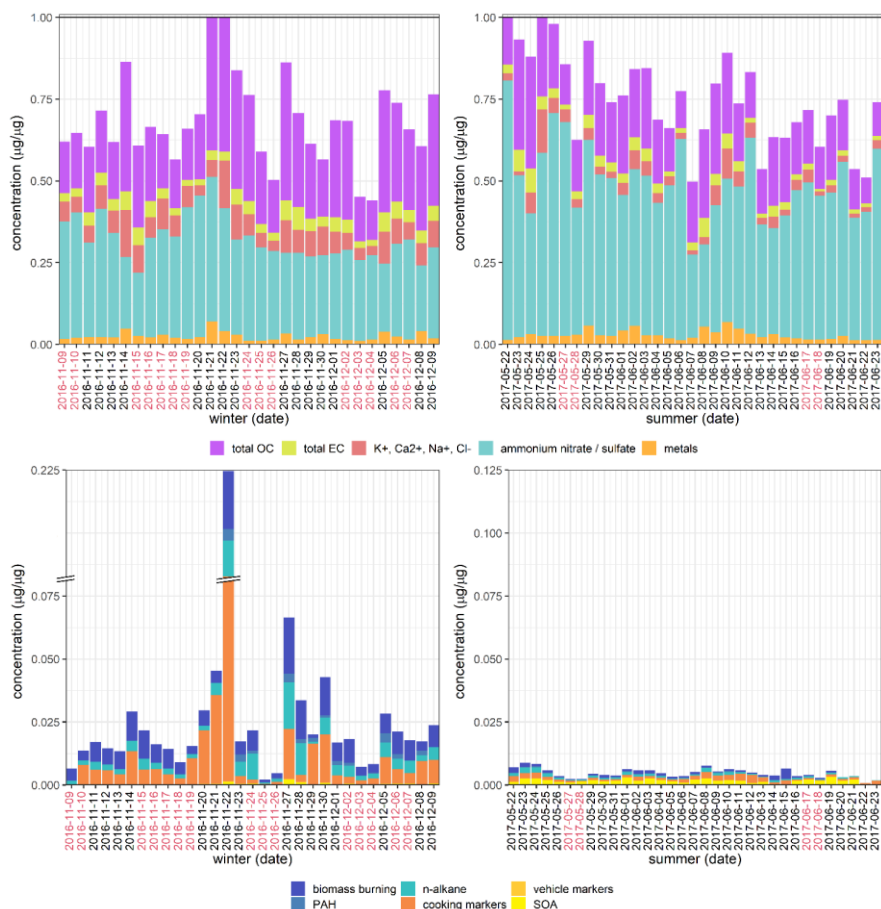


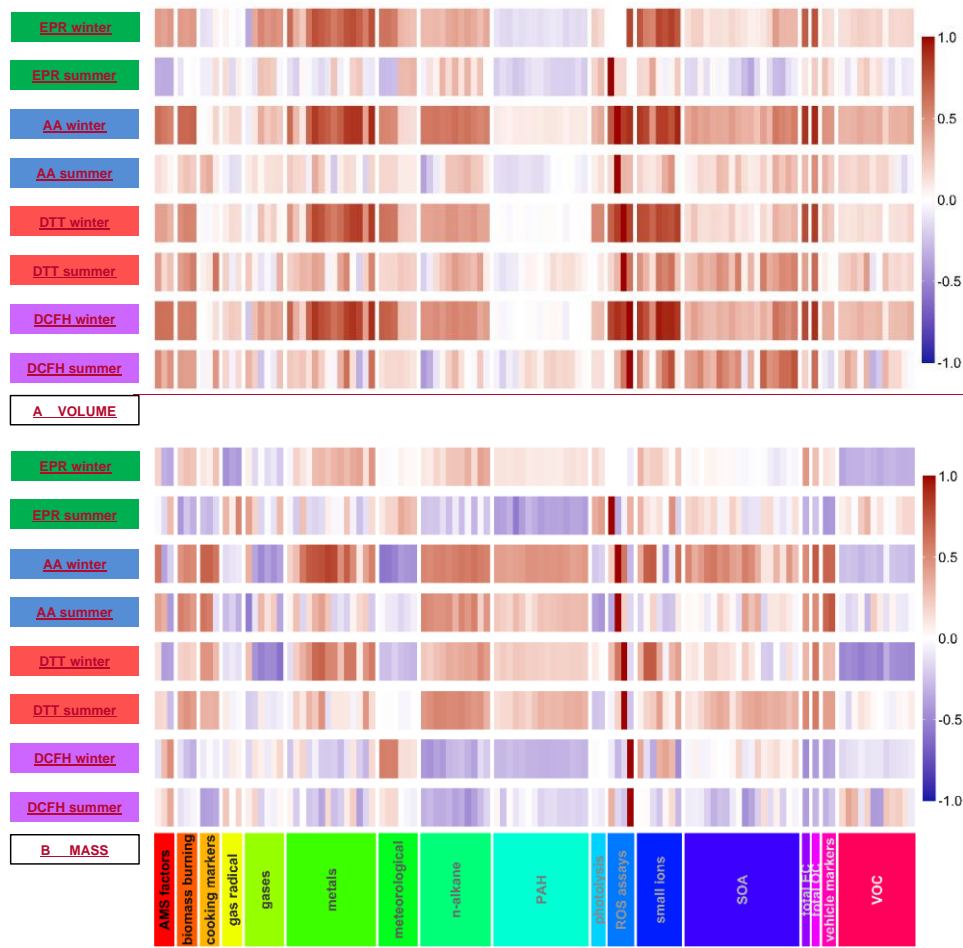
**Figure 4.** Stacked bar plots of total concentrations for mass-normalised data. **Abbreviations:** OC: organic carbon; EC: elemental carbon; PAH: polycyclic aromatic hydrocarbon; SOA: secondary organic aerosol “Metals” is the summed concentrations of Al, Ti, V, Cr, Mn, Fe, Co, Ni, Cu, Zn, Cd, Sb, Ba, Pb; “biomass burning” is the summed concentrations of palmitic acid, stearic acid and cholesterol; “PAH” is the summed concentrations of naphthalene, acenaphthylene, acenaphthene, fluorene, phenanthrene, fluoranthene, pyrene, benzo(a)anthracene, chrysene, benzo(b)fluoranthene, benzo(k)fluoranthene, benzo(a)pyrene, indeno(1,2,3-cd)pyrene, dibenzo(a,h)anthracene and benzo(ghi)perylene; “n-alkane” is the summed concentrations of C24, C25, C26, C27, C28, C29, C30, C31, C32, C33, C34; “cooking markers” is the summed concentrations of palmitic acid, stearic acid, cholesterol; “vehicle markers” is the summed concentrations of 17a(H)-22,29,30-trisnorhopane (C27a) and 17b(H),21a(H)-norhopane (C30ba); “SOA” is the summed concentrations of 2-methylthreitol, 2-methylerythritol, 2-methylglyceric acid, cis-2-methyl-1,3,4-trihydroxy-1-butene, -methyl-2,3,4-trihydroxy-1-butene, trans-2-methyl-1,3,4-trihydroxy-1-butene, C5-alkene triols, 2-methyltetrols, 3-hydroxyglutaric acid, cis-pinonic acid, acid, MBTCA, beta-caryophyllinic acid,

glutaric acid derivative, 3-acetylpentanedioic acid, 3-acetylhexanedioic acid, 3-isopropylpentanedioic acid and 2,3-dihydroxy-4-oxopentanoic acid. Dates marked in red indicate partial or total day haze events as described in Shi et al. (2019). Measurement uncertainty values were unavailable for most data types, and for selected dates in the upper plots, the sum of the total mass measurements is slightly more than 1 (i.e. more than 1 µg per µg); for these dates, the data has been proportionately scaled. It should be noted that the OC measurement in the upper plots incorporates the variety of organic carbon species represented in the lower plots.

$R_s$  calculated for  $OP_v$  and  $OP_m$  with the individual compositional measurements have strikingly different univariate correlations, as illustrated in correlation heatmaps (**Figure 5**). Cumulative scores, referring to the number of  $R_s$  correlations  $\geq 0.5$  for  $OP_m$  and  $OP_v$  (Table S3), demonstrate that for all assays, considerably more significant correlations are observed for  $OP_v$  in the winter compared to  $OP_m$ . For both  $OP_v$  and  $OP_m$ , all assays show more statistically significant correlations in winter compared to summer, particularly for the AA response ( $AA_m$ ,  $n = 54$  winter,  $n = 15$  summer,  $AA_v$ ,  $n = 67$  winter,  $n = 4$  summer).

Volume-based correlation analysis (**Figure 6A5A**) indicates that a very large number of the 107 atmospheric components measured in this study correlate statistically significantly with all four assays. The large number of correlations in the volume-normalised data indicate strong collinearity between concentrations of chemical components in  $PM_{2.5}$  and overall  $PM_{2.5}$  mass concentrations likely due to meteorological processes, complicating analysis of the sources and processes contributing to OP variability in particles. However, the mass-based analysis (**Figure 6B5B**) reveals that the mass fractions of chemical components and sources to which the four assays are sensitive to differ significantly (further illustrated by the weaker inter-assay correlations shown in Table 1), which demonstrates that mass-based analysis of OP data is also important to elucidate atmospheric processes and particle sources responsible for the different OP metrics.

480



485

**Figure 5.** Heatmaps demonstrating the correlation of OP, expressed as volume-normalised  $OP_v$  (A) and mass-normalised  $OP_m$  (B) vs a range of additional measurements conducted during the APHH campaign. Red indicates positive correlation; blue indicates inverse correlation. For  $OP_m$ , particle-phase components are also mass normalised ( $\mu\text{g per } \mu\text{g PM}_{2.5}$  and for  $OP_v$ , volume-normalised ( $\mu\text{g or ng per m}^3$ ).

A range of transition metals were all positively correlated with AA<sub>m</sub> and DTT<sub>m</sub>, including V, Cr, Mn, Fe, Co, Ni, Zn, Cd and Pb (all  $R_s \geq 0.5$ ,  $p < 0.05$ ). This reinforces the importance of their contribution to urban PM<sub>2.5</sub> and potential to ~~exert oxidative stress in tissues~~substantially influence PM<sub>2.5</sub> OP, particularly Fe, Cr, V and Co which are commonly major components of vehicle emissions, and which can undergo redox-cycling reactions producing ROS (Charrier et al., 2014; Shen and Anastasio, 2012; Valko et al., 2005) contributing to higher AA<sub>m</sub> and DTT<sub>m</sub> in the winter compared to the summer. Stronger correlations between Fe and AA<sub>m</sub> are observed in the winter ( $R_s$  0.73) compared to summer ( $R_s$  0.48) despite Fe concentrations ( $\mu\text{g}/\mu\text{g}$ ) being lower in winter samples than summer samples, again ~~high~~highlighting the enhanced role of redox-active transition metals in winter. It is not established whether this seasonal difference is related to the chemical availability (i.e. redox state, solubility, speciation) of Fe, to the variability of emission sources of Fe between the seasons, or to some other important unknown additional contribution of Fe to ROSAA<sub>m</sub> in the summer; complexation of ~~the~~Fe in PM may differ between seasons, and the ligands ~~can~~ directly influence the redox state and thus the bioavailability of the metal (Ghio et al., 1999). ~~Interestingly, a mild inverse correlation of Fe with DCFH<sub>m</sub> is observed (Table S8, not statistically significant)~~Ultimately, the direct correlation of transition metals measured only by ICP-MS with OP does not adequately reflect the nuances in redox behaviour of these species when they are complexed with organic ligands (Calas et al., 2017), as well as their range of oxidation states; this represents further gaps in the standard chemical (and particularly the transition metal) characterisation of PM. The epidemiological effects related to bioavailability of the metal when complexed (Costa and Dreher, 1997) in humans are also still not fully explored, although it is clear from multiple atmospheric and clinical studies that complexation affects both transition metal uptake in both the atmosphere and in the body. Interestingly, a mild inverse correlation of Fe with DCFH<sub>m</sub> is observed (Table S8), which may be linked to the destruction of particle-bound organic peroxides by Fe *via* Fenton-type chemistry (Charrier et al., 2014), a process which the DCFH assay is specifically sensitive to (Gallimore et al., 2017; Wragg et al., 2016), and which has been observed in other recent studies (Paulson et al., 2019). No significant positive correlation between any metals measured in this study and DCFH<sub>m</sub> and EPR<sub>m</sub> was observed. Few EPR studies have looked specifically at superoxide formation, as is the case here, but those conducted so far show that EPR specifically detecting O<sub>2</sub><sup>-</sup> is less sensitive to transition metal chemistry compared to traditional EPR methods focussing on OH formation.▲

**Formatted:** Font color: Custom Color(RGB(34;34;34)),  
Pattern: Clear (White)

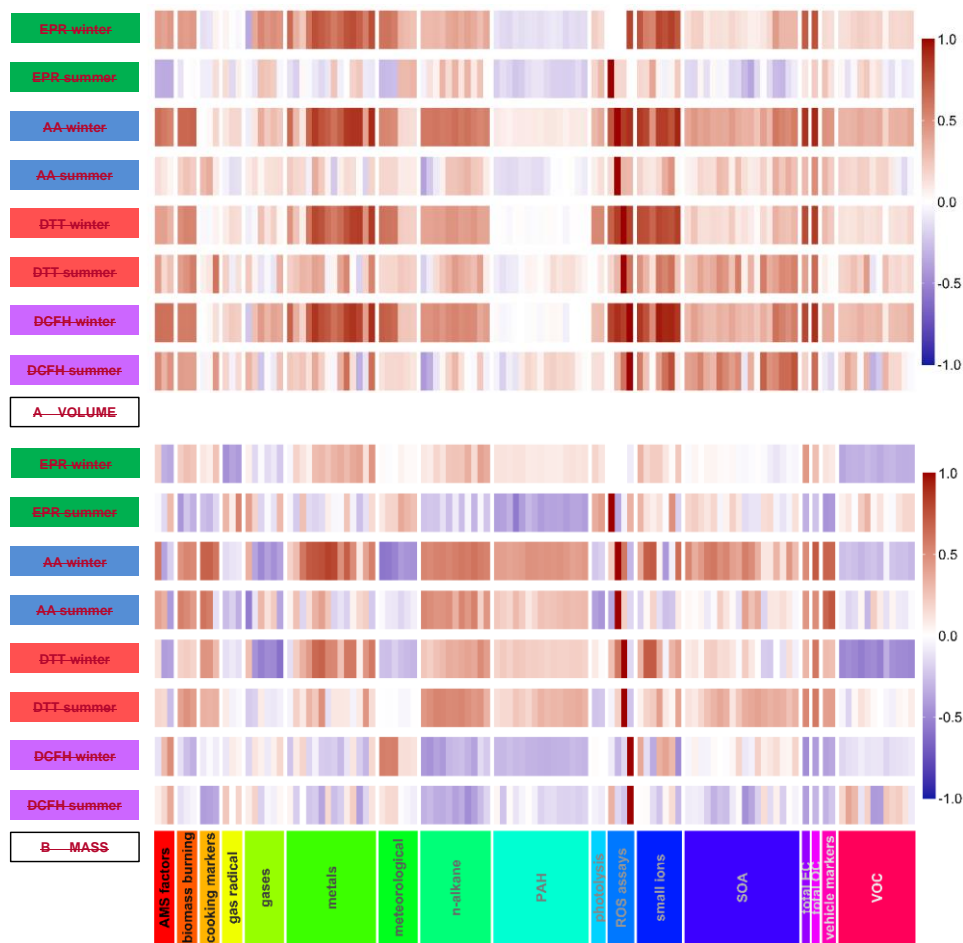


Figure 5. Heatmaps demonstrating the correlation of OP, expressed as volume normalised  $OP_v$  (A) and mass normalised  $OP_m$  (B) vs a range of additional measurements conducted during the APHH campaign. Red indicates positive correlation; blue indicates inverse correlation. For  $OP_m$ , particle-phase components are also mass normalised ( $\mu\text{g per } \mu\text{g PM}_{2.5}$  and for  $OP_v$ , volume normalised ( $\mu\text{g or ng per m}^3$ ).

In the summer, from the measured transition metals, only Fe correlated significantly positively (Spearman correlation p-value  $< 0.05$ ) with  $DTT_m$  and  $AA_m$  response ( $R_s = 0.48, 0.51$  respectively), whereas in the winter,  $DTT_m$  and  $AA_m$  correlated with a number of transition metals including V, Cr, Mn, Fe, Co, Ni, Zn, Cd. Of particular note,  $AA_m$  is mildly correlated with Cu in

Formatted: Space Before: 0 pt

winter samples ( $R_s$  0.48), whereas no correlation is observed between  $DTT_m$  and Cu in either winter or summer, in agreement with a recent online DTT study also (Puthussery et al., 2020). In contrast, previous reports from other locations have implicated Cu as a dominant contributor to DTT oxidation, considering volume normalised and mass normalised data (Calas et al., 2018; Charrier et al., 2015)(Calas et al., 2018; Charrier et al., 2015). Interestingly, in contrast with  $OP_m$ , strong correlations ( $R_s > 0.6$ ) are observed in this study between  $AA_v$ ,  $EPR_v$ ,  $DCFH_v$  and  $DTT_v$  and Cu in the winter, but poorer correlations are observed in the summer for all assays ( $R_s < 0.39$ ). Higher average Cu concentrations in winter compared to summer (winter =  $17.7 \text{ ng m}^{-3}$ , summer =  $4.9 \text{ ng m}^{-3}$ ) may explain the higher  $R_s$  observed for Cu vs.  $OP_v$  in winter compared to summer, whereas mass normalized concentrations of Cu are more similar between the seasons. Poor correlation of Cu concentrations with  $AA_m$  and  $DTT_m$  response in winter may hint at more insoluble Cu complex formation observed at this site in Beijing, as predominantly water-soluble Cu participates in redox reactions, therefore the sensitivity of AA and DTT towards Cu probably depends on the soluble fraction of Cu (Bates et al., 2019; Charrier and Anastasio, 2012; Fang et al., 2016)(Bates et al., 2019; Charrier and Anastasio, 2012; Fang et al., 2016). Furthermore, the presence of organic chelating ligands in PM may reduce the redox-activity of Cu and Fe (Charrier et al., 2014; Charrier and Anastasio, 2011; Shen and Anastasio, 2012).

Correlations between  $AA_m$  and  $DTT_m$  with total OC are observed in both summer and winter (Tables S6 and S7), and with total EC in the winter season, whereas  $DCFH_m$  is negatively correlated with total OC (Table S8). In contrast,  $DCFH_m$  is positively correlated with MOOOA and LOOOA, whereas  $DTT_m$  and  $AA_m$  show no correlation and even exhibit slight negative correlations with MOOOA and LOOOA in both summer and winter. This potentially indicates that the MOOOA and LOOOA AMS fractions, typically associated with water-soluble organic carbon content (Verma et al., 2015b), may contain higher concentrations of particle-bound ROS (i.e. organic peroxides) as measured by  $DCFH_m$ , but on a per-mass basis these species may contribute less significantly to  $AA_m$  and  $DTT_m$  compared to redox-active transition metals and other organic components. Total OC and EC correlations with  $AA_m$  and  $DTT_m$  may relate to concentrations of redox-active organic components such as oxidized PAHs and quinones, which may not be represented by MOOOA and LOOOA factors and which have been shown to significantly contribute to  $DTT_m$  (Chung et al., 2006; McWhinney et al., 2013b).

Significant correlations are also observed between  $AA_m$  and a range of *n*-alkanes and hopanes (17a(H)-22, 29,30-trisnorhopane (C27a) and 17b(H)-21a-norhopane (C30ba), Table S6), markers of primary organic aerosol emitted from vehicles (Schauer et al., 1999; Subramanian et al., 2006). Although these species are not redox-active, they are co-emitted with redox-active transition metals such as Fe, V and Cu from vehicle activity, either directly (Bates et al., 2019)(Bates et al., 2019) or via dust resuspension, and other organics contributing to SOA (Platt et al., 2014) and highlight the potential importance of vehicular emissions on  $AA_m$ . Vehicular emissions and dust-resuspension have been previously shown to be the dominant sources of Cu and Fe in Beijing (Gao et al., 2014).  $EPR_m$ ,  $DTT_m$  and  $DCFH_m$  responses do not show any significant correlations with these organic traffic markers.

Notably,  $AA_m$  correlates well with cis-pinonic acid, pinic acid and 3-methyl-2,3,4-butanetricarboxylic acid (MBTCA) in both seasons, all of which are biogenic SOA markers and products of  $\alpha$ -pinene oxidation, with MBTCA a marker for OH-initiated ageing of first generation  $\alpha$ -pinene oxidation products (Müller et al., 2012). AA sensitivity towards  $\alpha$ -pinene SOA has been



demonstrated previously (Campbell et al., 2019b)(Campbell et al., 2019a). Although these three carboxylic acids are also not redox-active, they may correlate with the formation of particle-bound ROS such as peroxides or peroxy acids in SOA (Steimer et al., 2018), or with species that decompose liberate ROS upon extraction (e.g. (Tong et al., 2017)); these processes are highly likely to contribute to AA<sub>m</sub>, highlighting the assay's potential sensitivity to redox-active particle phase organic-components and particle-bound ROS. Generally, DTT<sub>m</sub> has been previously shown to be relatively insensitive to SOA as observed here (Bates et al., 2015; Verma et al., 2015b)(Bates et al., 2015; Verma et al., 2015b), and both DTT<sub>m</sub> and DCFH<sub>m</sub> correlate poorly with the SOA markers analysed in the present study (Tables S7 and S8).

Compared to the three other assays, few significant correlations are observed between EPR<sub>m</sub> and additional measurements, despite the much better correlations with the EPR<sub>v</sub> data, particularly for the summer samples. However, seasonality in the EPR<sub>m</sub> response is still observed, with substantial variability in the mass-normalised EPR<sub>m</sub> response ( $\approx$  factor of 10 in the summer, factor of 2 in the winter, Figure 3Figure 3). Therefore, we observe differences in aerosol composition influencing EPR<sub>m</sub>, but with the current comprehensive measurements (i.e., 107 parameters) are unable to determine the specific PM<sub>2.5</sub> components responsible for the observed EPR<sub>m</sub> variation.

The univariate analysis presented here clearly shows that OP<sub>m</sub> enables a more nuanced identification of aerosol components linked to OPinfluencing the oxidising properties of PM<sub>2.5</sub> as compared to OP<sub>v</sub>. Many more correlations are observed when considering volume-normalised OP<sub>v</sub>, likely related to collinearity of species with overall PM<sub>2.5</sub> mass concentration due to meteorological effects. Metal and organic tracers of traffic emissions (exhaust and non-exhaust) such as Fe, Cu and hopanes and SOA markers show especially strong correlations with AA<sub>m</sub>, whereas the other three OP<sub>m</sub> metrics (DTT<sub>m</sub>, DCFH<sub>m</sub> and EPR<sub>m</sub>) provide a less clear picture.

### 3.3 Multivariate modelling of OP from measured components

To assess potential latent influences from the individual components on assay response and hence on OP, a systematic multivariate analysis was undertaken. Initially, principal components analysis was applied to the whole set of independent measurements excluding the OP assay responses (i.e. the values to be predicted by the models), to investigate which contributed most to the variation in the data, whether there were relationships between measurements which characterised OP, and if the OP<sub>m</sub> response could be predicted from the individual component measurements.

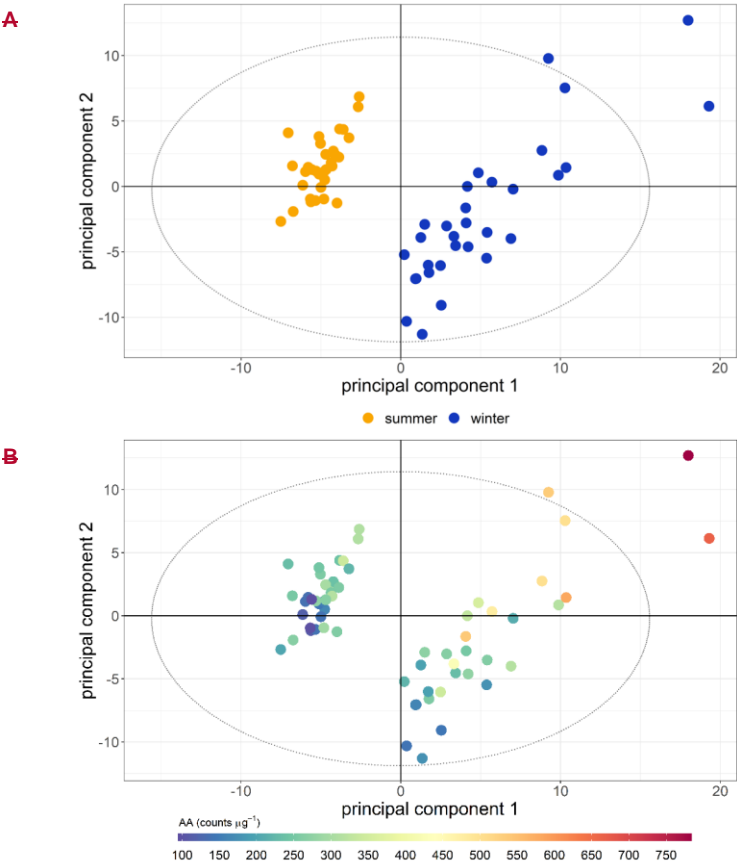
In the PCA model, the seasonal variation within the samples was clearly apparent (Figure 6). The first four principal components (PC) accounted for 68.2% of the observed variation in the dataset ( $R^2$  or goodness-of-fit), of which 50.5% was stable through 7-fold cross-validation ( $Q^2$ , or model variation accounted for through cross-validation), indicating about half of the variation in the model was robust with respect to sample score prediction. The loadings plot for this model (Figure 7) indicated the primary drivers of that seasonality in the first principal component werewas related to increased PAHs (Feng et al., 2019)(Feng et al., 2019), *n*-alkanes (He et al., 2006)(He et al., 2006) and biomass burning markers (He et al., 2006)(He et al., 2006) in winter, and increased ozone (Zhao et al., 2018)(Zhao et al., 2018), ambient temperature and selected SOA markers (including 2-methylerythritol (Liang et al., 2012)(Liang et al., 2012) and 2-methylglyceric acid (Ding et al., 2016;

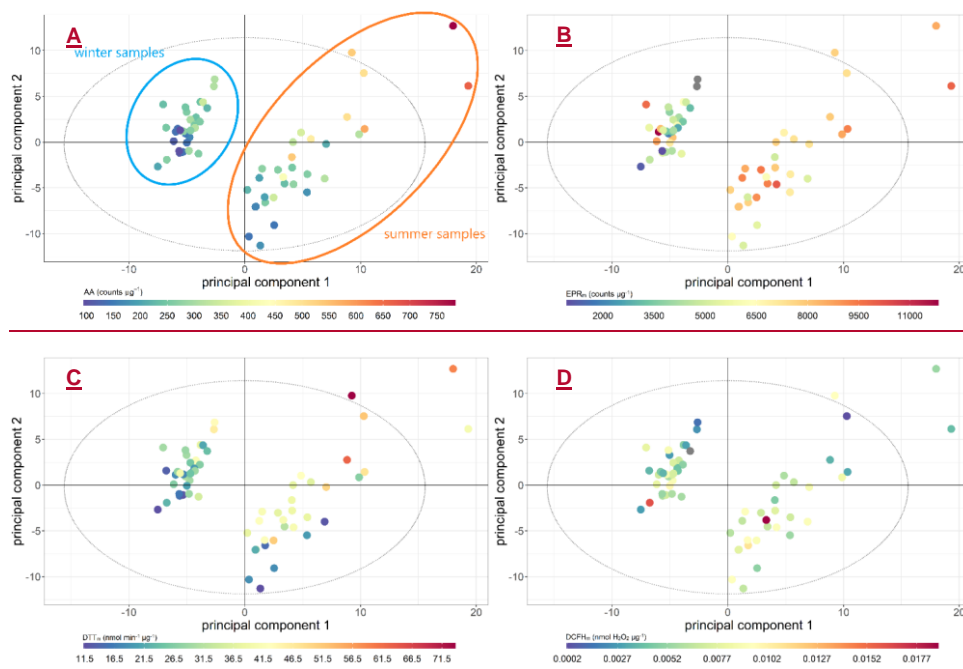
Formatted: Font: Bold

Formatted: French (France)

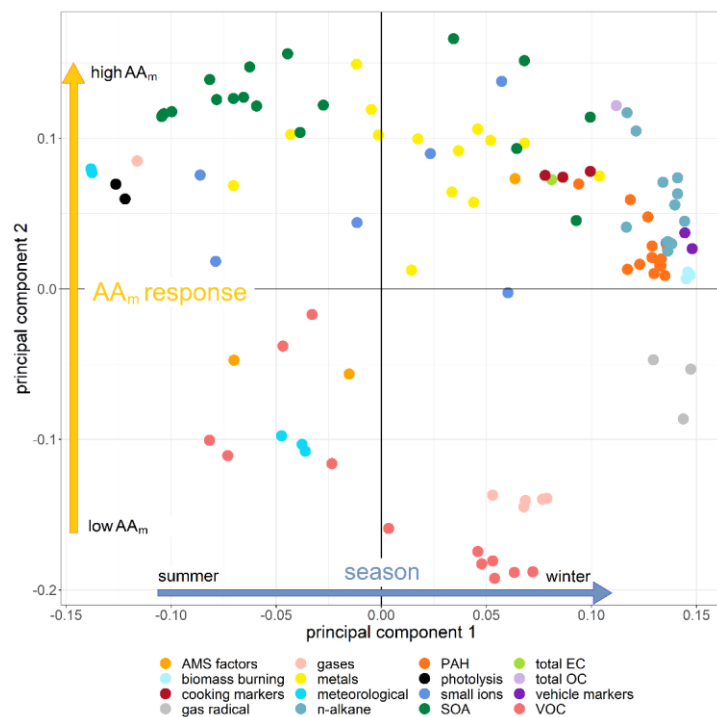
Formatted: French (France)

Shen et al., 2018)) in summer, findings which are consistent with existing volume-based studies. When scores were coloured by OP, the AA<sub>m</sub> (Figure 6B6A), DTT<sub>m</sub> (Figure 6C) and DCFH<sub>m</sub> (Figure 6D) assay responses could be observed in the second and sometimes also the first principal components (although the EPR<sub>m</sub> response demonstrated no specific trend, Figure S146B). When loadings plots were examined by general measurement category (Figure 7), it was observed some categories of measurements cluster together (e.g. PAH, *n*-alkanes, NO<sub>x</sub>, temperature, relative humidity), but this was related to strong correlation of these species with the OP<sub>m</sub> measurement and known compound behaviour rather than to intrinsic-measurement bias, as other categories showed broader variation (e.g. inorganic and small organic ions, gases, metals and SOA markers).





**Figure 6.** Principal components analysis scores plot of all data. A: coloured by season (winter/summer)-AA<sub>m</sub> response; B: coloured by AA<sub>m</sub> response-EPR<sub>m</sub> response; C: coloured by DTT<sub>m</sub> response; D: coloured by DCFH<sub>m</sub> response. Both principal component 1 and principal component 2 demonstrate variance associated with AA and DTT response, and there is greater variation associated with the winter response than the summer response- (highlighted in A). PC 1 R<sup>2</sup>X 35.90%, Q<sup>2</sup> 29.28%; PC 2 R<sup>2</sup>X 19.34%, Q<sup>2</sup> 23.73%; the model included six principal components, with a cumulative R<sup>2</sup>X of 68.2% and Q<sup>2</sup> of 50.5%. Analogous colour-coded PCA plots for DTT<sub>m</sub>, DCFH<sub>m</sub> and EPR<sub>m</sub> are shown in Figures S14-S16.



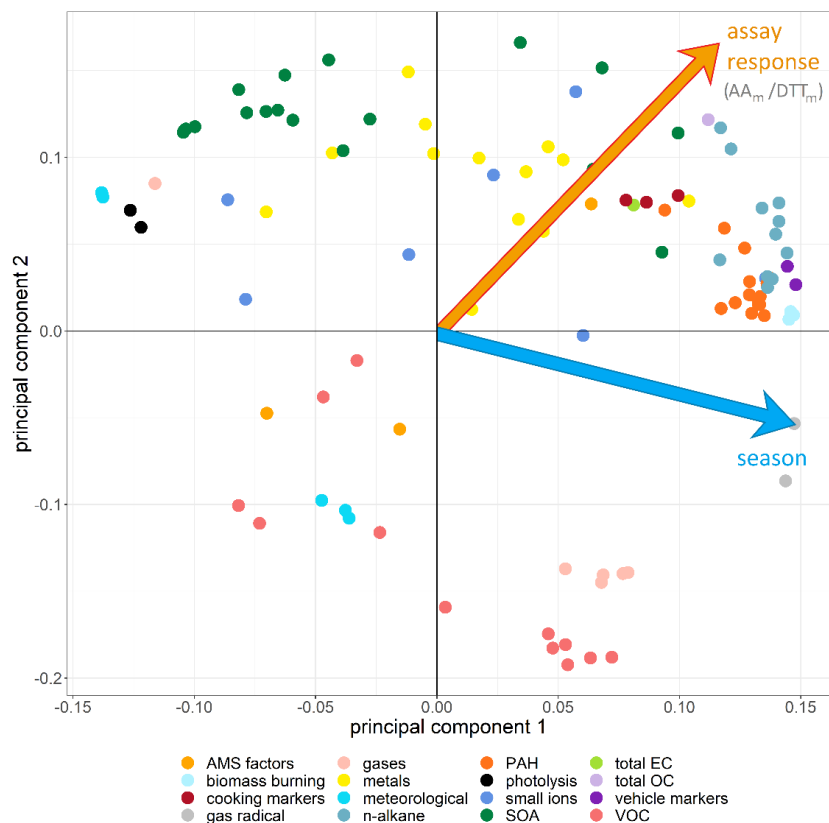


**Figure 7.** Principal components analysis loading plot for all data points. Points are coloured by measurement category; a fully labelled plot is provided in Figure S17S14. The plot is annotated with the same orientation as the scores plot, to indicate the direction of visualised trends in Figure 6 for selected assays and for season from the latent variable origin as shown in Figure 6. In PC 1, the winter classification is driven by increased gas radicals, *n*-alkanes, PAH, vehicle markers, biomass burning markers, total OC and selected metals and SOA markers; the summer classification is driven by increased temperature and photolysis, ozone (the single gas species in this section of the plot), selected SOA markers and metals, and selected VOCs. In PC 2, high  $AA_m$  and  $DTT_m$  response is associated with increased SOA, transition metals, cooking markers, *n*-alkanes and PAH concentrations in samples; low  $AA_m$  and  $DTT_m$  response associated with low VOCs, gases and selected meteorological parameters (relative humidity).

Partial least squares regression (PLSR) is a supervised regression extension of PCA, which models the variation in the data associated with a defined sample classification (Eriksson et al., 2013). PLSR models were constructed for each individual OP

assay and season, to examine the most specific markers associated with assay response. **Table 2** gives provides the model performances for all PLSR assay models, and example PLSR scores plots for AA<sub>m</sub> and DTT<sub>m</sub> models (both seasons) are illustrated in **Figures 8 and 9** (analogous plots for other assays provided in **Figures S18 and S19**). The performance indicators show that while the mass-normalised measurement data can be used to explain and predict a large majority of the variation associated with AA<sub>m</sub> summer/winter and DTT<sub>m</sub> winter assay response, the other assay responses were less consistent; R<sup>2</sup> and Q<sup>2</sup> values for these models indicated that less than 70% of the variance in response can be predicted from the individual component measurements, and the predictions were much less stable through cross-validation. These results could suggest either that assay responses are not as adequately sensitive at the µg/µg concentrations as for the total volume of PM per sample, or that a proportion of the OP<sub>m</sub> response is contributed to by species not measured directly in this campaign; and which cannot also be inferred from total organic carbon measurements. As total OC is estimated from combustion properties of the sample rather than from a sum of individually validated component measurements, and as multiple organic and transition metal-organic complexed species contribute to the total OC measurements with unknown redox properties, these observations highlight the need for more comprehensive chemical characterisation of PM composition. Similarly to the univariate correlations, the summer samples were less well modelled in both mass-normalised and volume-normalised data, indicating either reduced assay sensitivity (which may also be compounded by the reduced collected filter PM mass in summer) or the influence of unmeasured components.

**Table 2.** Performance assessment of PLSR models for all assays, for both mass-normalised (left) and volume-normalised (right) data. Models are considered to perform well when both cumulative (i.e. across all latent variables included in the model) R<sup>2</sup> and Q<sup>2</sup> values are high, or at a minimum where Q<sup>2</sup> values are within 10% of the R<sup>2</sup> value, indicating that the variance is well accounted for in model cross-validation. Permutation tests were rejected for robustness if any single random permutation model performance surpassed the performance of the real cross-validated model; on this basis, the winter DCFH<sub>m</sub> and summer DTT<sub>v</sub> models were rejected (highlighted with \*), although fewer than three random models outperformed the real model, and none of the permuted model Q<sup>2</sup> values outperformed those of the real model.

assay	season	mass (µg/µg)				volume (µg/m <sup>3</sup> )			
		optimal	cumul.	cumul.	permutation	optimal	cumul.	cumul.	permutation
		LVs	<del>cumulative</del> R <sup>2</sup>	<del>cumulative</del> Q <sup>2</sup>		LVs	<del>cumulative</del> R <sup>2</sup>	<del>cumulative</del> Q <sup>2</sup>	
EPR	winter	1	43.2	19.3	no	2	83.9	75.2	yes
	summer	1	11.3	-10.0	no	1	52.0	3.7	no
AA	winter	1	81.4	78.2	yes	2	94.1	87.9	yes
	summer	2	79.3	49.7	yes	1	41.8	22.6	no
DTT	winter	2	76.0	62.0	yes	2	86.8	67.0	yes
	summer	1	47.4	31.6	no	1	66.2	50.9	no*
DCFH	winter	2	71.9	50.4	no*	2	67.0	55.2	yes
	summer	1	28.2	-6.6	no	1	86.0	66.7	yes

Formatted Table

Formatted Table

Formatted Table

Formatted Table

Formatted Table

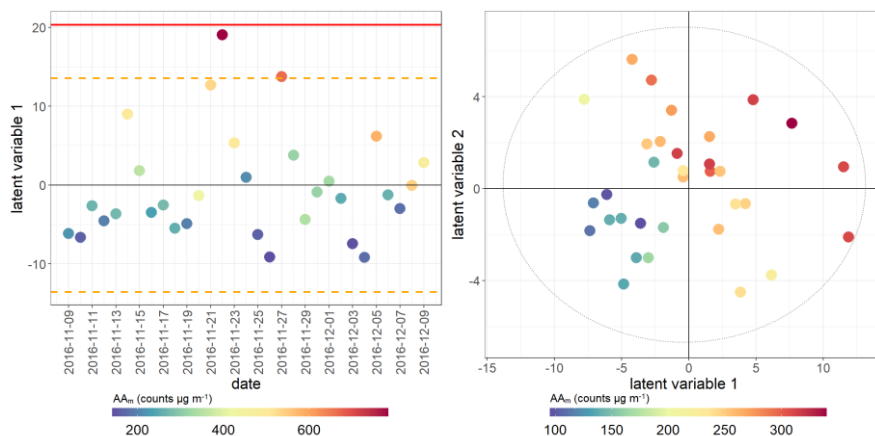


**Figure 8.** PLSR scores plot for  $AA_m$  assay. Model performance parameters given in Table 2. Left: winter samples; right: summer samples. Points coloured by overall AA assay response for both seasons. Red bar indicates  $2 \times SD$  for all scores, orange dotted line indicates  $1 \times SD$  for all scores. Models which have only one latent variable have the X-axis replaced by date for easier visualisation.

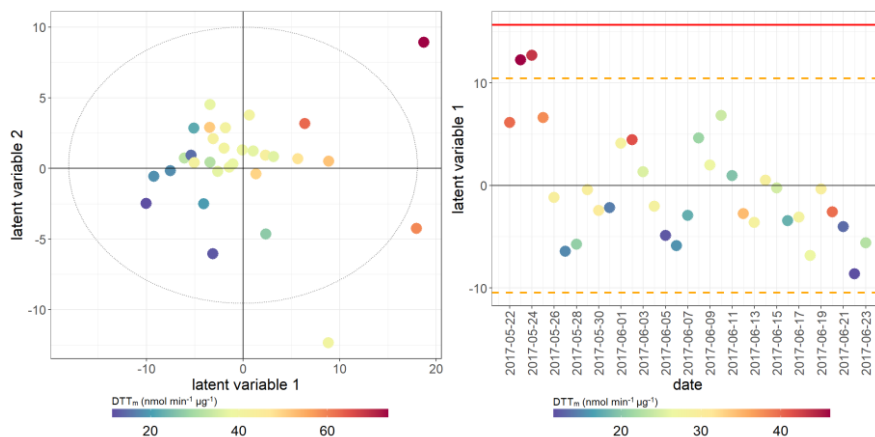


**Figure 9.** PLSR scores plot for  $DTT_m$  assay. Model performance parameters given in Table 2. Left: winter samples; right: summer samples. Points coloured by overall DTT assay response for both seasons.

**Table 3**

655

**Table 3.** Characteristic loadings most influential in PLSR models of OP<sub>m</sub> as defined by ordered variable importance in projection for each model. Blue upward arrows indicate positive correlation with the assay measurement, red downward arrows for inverse correlation, and \* for p < 0.05 in Spearman correlation of the feature with the assay in the univariate analysis.

EPR <sub>m</sub> winter		AA <sub>m</sub> winter		DTT <sub>m</sub> winter		DCFH <sub>m</sub> winter	
feature	VIP	feature	VIP	feature	VIP	feature	VIP
indeno[1,2,3-cd]-pyrene *	2.12 ↑	cis-pinonic acid *	1.44 ↑	SO <sub>2</sub> *	1.46 ↓	NH <sub>4</sub> <sup>+</sup>	2.16 ↑
acenaphthylene	2.02 ↑	Cl <sup>-</sup>	1.42 ↑	Ca <sup>2+</sup> *	1.40 ↑	chrysene *	1.61 ↓
benzo[ghi]-perylene *	2.01 ↑	total OC *	1.33 ↑	Fe *	1.37 ↑	benzo[b]-fluoranthene *	1.59 ↓
benzo[a]pyrene *	2.01 ↑	MOQOA *	1.30 ↑	fluorene	1.34 ↑	RH8 *	1.59 ↑
fluorene	1.82 ↑	pyrene *	1.30 ↑	acetaldehyde *	1.33 ↓	benzo[a]anthracene *	1.58 ↓
benzo[a]-anthracene *	1.81 ↑	2-methylthreitol	1.29 ↑	phenanthrene *	1.33 ↑	pyrene *	1.58 ↓
dibenzo[a,h]-anthracene *	1.80 ↑	ORG *	1.29 ↑	acetone *	1.33 ↓	LOQOA *	1.57 ↑
phenanthrene *	1.77 ↑	benzo[k]-fluoranthene *	1.29 ↑	Cl <sup>-</sup>	1.31 ↑	fluoranthene *	1.56 ↓
chrysene *	1.66 ↑	3-methyl-2,3,4-trihydroxy-1-butene *	1.28 ↑	benzene *	1.31 ↓	RH120 * / RH240 *	1.55 ↑
naphthalene *	1.62 ↑	fluoranthene *	1.27 ↑	toluene *	1.30 ↓	K <sup>+</sup> *	1.51 ↑

EPR <sub>m</sub> summer		AA <sub>m</sub> summer		DTT <sub>m</sub> summer		DCFH <sub>m</sub> summer	
feature	VIP	feature	VIP	feature	VIP	feature	VIP
LOQOA	2.59 ↑	ORG *	1.80 ↑	OH	1.58 ↑	cis-pinonic acid *	2.38 ↓
T8 / T120 / T240	2.28/2.15/2.08 ↑	cis-pinonic acid *	1.62 ↑	dibenzo[a,h]-anthracene *	1.51 ↑	C31 *	1.76 ↓
O <sub>3</sub>	2.00 ↑	MOQOA *	1.58 ↑	C26 *	1.48 ↑	pinic acid *	1.74 ↓
RO <sub>2</sub> *	1.76 ↑	cholesterol	1.58 ↓	benzo[a]-pyrene *	1.48 ↑	acetonitrile *	1.69 ↑
galactosan *	1.74 ↓	naphthalene *	1.57 ↑	total OC *	1.46 ↑	3-methyl-2,3,4-trihydroxy-1-butene	1.65 ↓
K <sup>+</sup>	1.70 ↑	palmitic acid *	1.49 ↑	C30 *	1.46 ↑	benzo[ghi]-perylene	1.62 ↓
17a(H)-22,29,30-trisnorhopane (C27a)	1.55 ↓	RH8	1.39 ↓	C28 *	1.43 ↑	C32	1.61 ↓
cis-2-methyl-1,3,4-trihydroxy-1-butene	1.55 ↑	stearic acid *	1.39 ↑	benzo[ghi]-perylene *	1.41 ↑	dibenzo[a,h]-anthracene *	1.61 ↓
Ba	1.47 ↓	benzo[ghi]-perylene *	1.36 ↑	C33 *	1.40 ↑	acetaldehyde *	1.61 ↑
RH8	1.46 ↓	benzo[a]-pyrene *	1.34 ↑	C29 *	1.39 ↑	isoprene *	1.61 ↓

Formatted Table

Formatted Table

Formatted Table

Formatted Table

Formatted: Justified, Space Before: 12 pt, Line spacing: 1.5 lines

Formatted: Font: Bold



660 **Table 3** shows the top ten features in the variable importance in projection (VIP) for the PLSR loadings, which enable a ranking of the features which contribute most to the model (Naes and Martens, 1988). It is evident from these data that the features which best model the OP<sub>m</sub> seasonal response are derived from multiple particle sources and atmospheric aging processes. For example, the AA<sub>m</sub> and DTT<sub>m</sub> responses show similar trends in the multivariate models, but the main contributors to their responses have little overlap, with AA<sub>m</sub> responses being more strongly associated with SOA tracers, PAHs and general measures of organic carbon, and the DTT<sub>m</sub> more characterised by combustion and vehicle emissions markers (**Figure 10**). **Figures S19-S22; Figures S17-S24 list the top 50 contributors to each assay model response**. Notably, compounds which are not generally recognised as being redox-active were frequently observed to be important in PLSR classification, and though they do not directly contribute to the OP<sub>m</sub> response, they are likely co-emitted with or are secondary products of redox-active particle components.

665 **Table 3.** Characteristic loadings most influential in PLSR models of OP<sub>m</sub> as defined by ordered variable importance in projection for each model. Blue upward arrows indicate positive correlation with the assay measurement, red downward arrows for inverse correlation, and ± for p < 0.05 in Spearman correlation of the feature with the assay in the univariate analysis.

EPR <sub>m</sub> -winter		AA <sub>m</sub> -winter		DTT <sub>m</sub> -winter		DCFH <sub>m</sub> -winter	
feature	VIP	feature	VIP	feature	VIP	feature	VIP
indeno(1,2,3-cd)-pyrene±	2.12↗	cis-pinonic-acid±	1.44↗	SO <sub>4</sub> ±	1.46↘	NH <sub>4</sub> ±	2.16↗
acenaphthylene	2.02↗	Cr±	1.42↗	Ca <sup>2+</sup> ±	1.40↗	chrysene±	1.61↘
benzo(ghi)-perylene±	2.01↗	total-OC±	1.33↗	Fe±	1.37↗	benzo(b)-fluoranthene±	1.59↘
benzo(a)pyrene±	2.01↗	MOOGA±	1.30↗	fluorene	1.34↗	RH8±	1.59↗
fluorene	1.82↗	pyrene±	1.30↗	acetaldehyde±	1.33↘	benzo(a)-anthracene±	1.58↘
benzo(a)-anthracene±	1.81↗	2-methylthreitol	1.29↗	phenanthrene±	1.33↗	pyrene±	1.58↘
dibenzo(a,h)-anthracene±	1.80↗	ORG±	1.29↗	acetone±	1.33↘	LOOGA±	1.57↗
phenanthrene±	1.77↗	benzo(k)-fluoranthene±	1.29↗	Cr±	1.31↗	fluoranthene±	1.56↘
chrysene±	1.66↗	2-methyl-2,3,4-trihydroxy-1-butene±	1.28↗	benzene±	1.31↘	RH120±/RH240±	1.55↗
naphthalene±	1.62↗	fluoranthene±	1.27↗	toluene±	1.30↘	K <sup>+</sup> ±	1.51↗

EPR <sub>m</sub> -summer		AA <sub>m</sub> -summer		DTT <sub>m</sub> -summer		DCFH <sub>m</sub> -summer	
feature	VIP	feature	VIP	feature	VIP	feature	VIP
LOOGA	2.59↗	ORG±	1.80↗	OH	1.58↗	cis-pinonic-acid±	2.38↘
T8/T120/T240	2.28/2.15/2.08↗	cis-pinonic-acid±	1.62↗	dibenzo(a,h)-anthracene±	1.51↗	Cr±	1.76↘
O <sub>2</sub>	2.00↗	MOOGA±	1.58↗	C26±	1.48↗	pinic-acid±	1.74↘
RO <sub>2</sub> ±	1.76↗	cholesterol	1.58↘	benzo(a)-pyrene±	1.48↗	acetonitrile±	1.69↗
galactosan±	1.74↘	naphthalene±	1.57↗	total-OC±	1.46↗	2-methyl-2,3,4-trihydroxy-1-butene	1.65↘
K <sup>+</sup>	1.70↗	palmitic-acid±	1.49↗	Cr±	1.46↗	benzo(ghi)-perylene	1.62↘
17a(H)-22,29,30-trisnorhopane (C27a)	1.55↘	RH8	1.39↘	C28±	1.43↗	Cr±	1.61↘
cis-2-methyl-1,3,4-	1.55↗	stearic-acid±	1.39↗	benzo(ghi)-	1.41↗	dibenzo(a,h)-	1.61↘

Formatted: Font: 10 pt

Formatted Table

Formatted Table

Formatted Table

Formatted Table

trihydroxy-1-butene				perylene±		anthracene±	
Ba	1.47 ±	benzo(ghi)perylene±	1.36 ±	C33±	1.40 ±	acetaldehyde±	1.61 ±
PH8	1.46 ±	benzo(a)pyrene±	1.34 ±	C29±	1.39 ±	isoprene±	1.61 ±

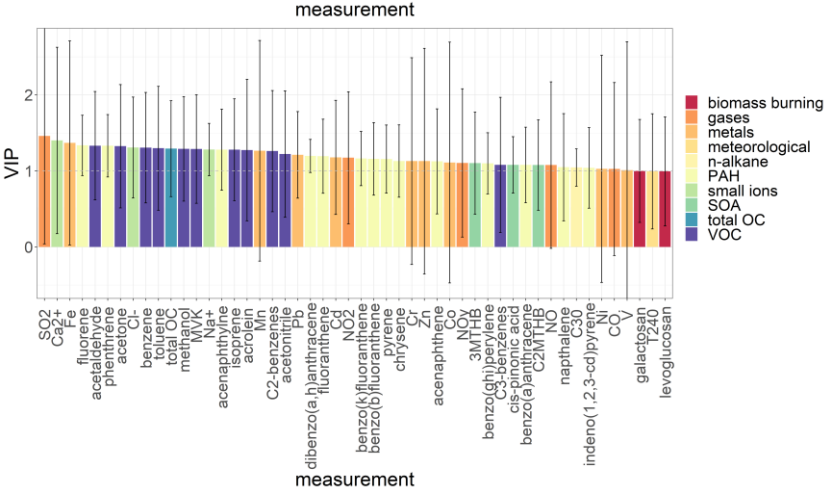
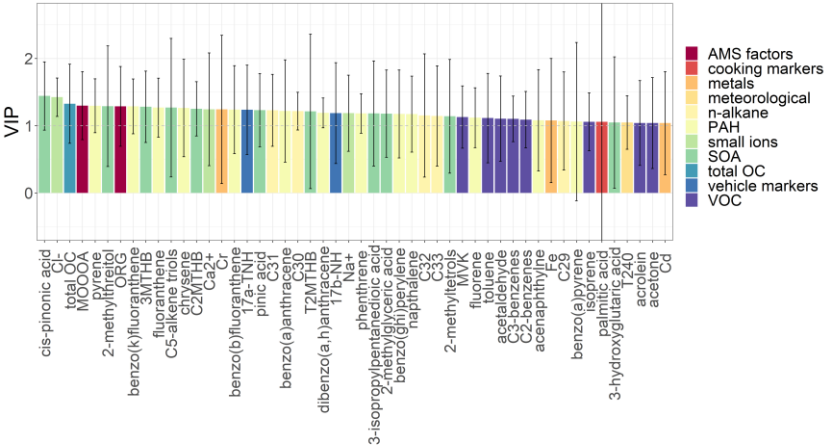


**Figure 10.** Variable importance in projection (VIP) plots. Above: winter AA<sub>m</sub> PLSR model; below: winter DTT<sub>m</sub> PLSR model (top 50 features only). Error bars represent the standard error of the mean for each feature and are often large due to the intrinsic noisiness and instability of the individual measurements. Terms with VIP > 1 contribute most significantly to the model. **Abbreviations:** 3MTHB: 3-methyl-2,3,4-trihydroxy-1-butene; C2MTHB: cis-2-methyl-1,3,4-trihydroxy-1-butene; T2MTHB: trans-2-methyl-1,3,4-trihydroxy-1-butene; 17a-TNH: 17a(H)-22,29,30-trisnorhopane (C27a); 17b-NH: 17b(H),21a(H)-norhopane (C30ba); MVK: methyl vinyl ketone or methacrolein. Analogous plots for all other assays are given in **Figures S20-S27**.

### 3.4 Multiple Linear Regression (MLR) modelling to predict OP<sub>m</sub> associated with specific sources

While multivariate model loadings highlighted the measurements most associated with assay response, ~~they do~~ multivariate models are not enable straightforward always amenable to variable selection, which is important to characterise the specific compounds chemical profiles contributing to each assay OP response. Multiple linear regression modelling has been used in previous studies (Calas et al., 2018)(Calas et al., 2018) to establish important contributors to total OP response, rather than looking at source apportionment in relation to OP, and only simple forward variable selection was used for model refinement. HereIn the present study, relevant measurements were grouped into six categories of known contributors to Beijing PM (biogenic SOA, biomass burning, coal and fossil power generation, cooking, dust and vehicle emissions). The full method description, references, model formulae and performance parameters for the mass-normalised data models are presented in the Methods (Section 2.3 “Statistical analysis”) and in Section S10. Briefly, literature sources (Table S13, Section S10) and the SPECIEUROPE database (Pernigotti et al., 2016) were used to establish which individual chemical measurements were likely to be characteristic of each source, with several measurements appearing in multiple categories (e.g. total EC). All proxy and composite measurements (except total EC, as numerous multiple organic carbon species are represented in the dataset, but elemental carbon should be independent of most the majority of these), AMS measurements, and general atmospheric measurements including temperature, relative humidity and actinic flux measurements were excluded from models entirely, as the composite. Composite measures duplicate selected individual measurements and the; atmospheric measurements complicate model interpretation, and are more likely to be useful as random effects terms in a mixed effects model approach (not pursued in the present study due to the complexity of model parameterisation and measurement uncertainties). Multiple linear regression models were then constructed for each assay and season for each category, using both mass-normalised and volume-normalised data.

MLR models further reinforced that not all putative sources and components of PM<sub>2.5</sub> contribute equally to OP<sub>m</sub> response (Table 4). OP<sub>m</sub> response models based on measurements characteristic of vehicle emissions, coal/fossil fuel combustion and biomass burning gave accurate and robust predictions of particle-level OP<sub>m</sub>, which are important contributors to PM (mass per volume) in Beijing urban background sites (Yu et al., 2013; Zheng et al., 2005). As expected, OP<sub>v</sub> models gave very good predictions for these source profiles, but also gave improved models of OP<sub>v</sub> for biogenic SOA and dust compared with the mass-normalised data. Although the same base sets of predictor measurements for each source were used for each type of model (season, OP and PM normalisation), there was only partial overlap of predictors between models from the same source and season, again illustrating the complex dynamic between OP and overall mass/volume composition. As with the PLSR models, the most important contributors to regression models were often not redox-active species, indicating that they could

710 be influencing or contributing to the oxidation state of the redox-active PM components, either through co-emission,  
propagation reactions or by direct oxidation of the species themselves. As with the univariate and multivariate analyses, the  
summer samples gave less robust linear regression models (and thus OP predictions) from both mass- and volume-normalised  
data. However, AA and DTT measurements produced the best subset modelling for all source panels, indicating that these  
assays might be most optimal for measuring OP in an urban environment, as they appear to reflect the variety of PM sources  
715 well.

▲  
▲  
**Table 4.** OP<sub>m</sub> assay response models based on measurements characteristic of vehicle emissions, coal/fossil fuel combustion  
and biomass burning gave accurate and robust predictions of OP<sub>m</sub>, and these are important contributors to PM (reported as  
720 mass per volume) in Beijing urban background sites (Yu et al., 2013; Zheng et al., 2005). As expected, OP<sub>v</sub> models also gave  
very good predictions for these source profiles, but additionally gave improved models of OP<sub>v</sub> for biogenic SOA and dust  
compared with the OP<sub>m</sub> data. Although the same base sets of predictors for each source were used for each model (season, OP  
assay and PM normalisation), there was only partial overlap of the final selected predictors between models from the same  
source and season, again illustrating the complex dynamic between OP and overall mass/volume composition. As with the  
725 PLSR models, the most important contributors to regression models were often not redox-active species, indicating that they  
are probably influencing or contributing to the oxidation state of the redox-active PM components. As with the univariate and  
multivariate analyses, the summer samples gave less robust linear regression models (and thus OP predictions) from both  
mass- and volume-normalised data. However, AA and DTT measurements produced the best models for all source  
contributions, indicating that these assays might be most optimal for measuring OP in an urban environment, as they appear  
730 to reflect the variety and composition of PM sources well.

Vehicle emissions, biogenic SOA and winter biomass burning contributions to AA and DTT response (as measured by the  
model R<sup>2</sup> value) were generally comparable across ~~all~~both assays, contrasting with the findings of ~~Fang et al. (2016)~~Fang et  
al. (2016), who observed greater OP response in positive matrix ~~factorization~~factorisation-chemical mass balance (PMF-CMB)  
models associated with traffic emissions for AA<sub>v</sub> over DTT<sub>v</sub>, and biomass burning for DTT<sub>v</sub> over AA<sub>v</sub> in multiple locations in  
735 the southeastern US. However, a more recent study conducted in the coastal areas adjacent to Beijing (~~Liu et al., 2018~~)(Liu et  
al., 2018) observed similar seasonality to the present study in the ~~DTT<sub>m</sub>-OP~~DTT OP<sub>m</sub> response. Vehicle emissions (Wang et  
al., 2016; Yu et al., 2019), coal combustion (Ma et al., 2018; Yu et al., 2019), biomass burning (Ma et al., 2018) and dust (Yu  
et al., 2019) sources have been shown in other studies using PMF models to contribute to OP<sub>v</sub> in Beijing, all using the DTT  
assay. Cooking markers (palmitic acid, stearic acid and cholesterol) contributed a substantial proportion of the known organic  
740 fraction of the PM mass and volume concentrations (see **Figure 4**), but did not contribute robustly to the modelled OP response  
for either normalisation type, suggesting they are either not strongly contributing to or affected by oxidative conditions in PM,  
or that their variation over the sampling period cannot be linearly modelled. Similarly, biomass burning markers contribute a  
comparable number of variables in the model base sets, but appear to contribute much more significantly to the OP<sub>v</sub> than to

Formatted: Font: Bold

Formatted: Font: 10 pt

the OP<sub>m</sub> response. Biogenic SOA and dust models (which incorporate K<sup>+</sup>, Na<sup>+</sup>, Ca<sup>2+</sup>, Cl<sup>-</sup>, Al, Ti, Mn, Fe and Zn) ~~explain~~explained a significant proportion of winter OP<sub>v</sub> responses, but ~~are~~were only strongly correlated with winter AA and DTT for mass-normalised models. ~~This suggests~~These observations suggest these sources contribute to PM OP<sub>v</sub> by total quantity rather than through their particularly high intrinsic OP<sub>m</sub>/OP<sub>v</sub>, i.e. their mass as a proportion of the PM mass is smaller, but ~~the number of particles~~their concentration per volume is ~~greater~~higher, and the AA and DTT assays have a ~~higher sensitivity~~notable selectivity for these species over the EPR and DCFH assays.

It should be noted that the MLR models represent a sub-optimal prediction of the OP response from measured components, as numerous species which are known source components (e.g. PAH in PAHs from combustion processes and distinguishing those which distinguish gasoline from diesel ~~vehicles, vehicle emissions, or~~ VOCs ~~is irrelevant to~~ biomass burning such as methanol or acrolein) could not be included in models. Not all measurements which were associated in the literature with a particular assay response passed the stages of variable selection for mass-normalised models, which could reflect a lower limit of detection in either the OP<sub>m</sub> assay responses, or in the individual component measurements. Moreover, Synergistic effects between individual measured components (e.g. transition metals with organic components such as quinones or carboxylic acids (Wang et al., 2018)) cannot be interpreted from linear models when the complexation and oxidation states of the contributing compounds are essentially unknown. MLR models do not fully account for the proportion of each measurement which may originate from multiple emissions sources, and PMF-CMB or mixed effects models ~~would can~~ address this issue more adequately. Validation of both the multivariate and MLR models using secondary datasets (both from Beijing and other ~~local~~ locations) is also needed prior to their future implementation.

**Table 4.** R<sup>2</sup> values for optimised subset multiple linear regression models of relevant source contributions. R<sup>2</sup> values greater than 0.7 are highlighted in bold. Full model performance indicators are provided in [Section S8S11](#) of the SI, including all model terms, residuals information, coefficients and p-values.

		EPR R <sup>2</sup>		AA R <sup>2</sup>		DTT R <sup>2</sup>		DCFH R <sup>2</sup>	
$\alpha$	$\beta$	winter	summer	winter	summer	winter	summer	winter	summer
HS/HS	vehicle emissions	0.88	0.72	0.95	0.73	0.91	0.80	0.89	0.62
HS/HS	biomass burning	0.41	0.29	0.49	0.47	0.45	0.41	0.58	0.31
HS/HS	coal/fossil fuel combustion	0.84	0.56	0.88	0.61	0.86	0.68	0.75	0.71

$\mu\text{g}/\mu\text{g}$	cooking markers	0.19	0.11	0.66	0.20	0.39	0.36	0.08	0.24
$\mu\text{g}/\mu\text{g}$	dust	0.23	0.23	0.88	0.47	0.72	0.46	0.50	0.26
$\mu\text{g}/\mu\text{g}$	biogenic SOA	0.55	0.35	0.95	0.74	0.79	0.61	0.55	0.70
$\mu\text{g}/\text{m}^3$	vehicle emissions	0.94	0.79	0.97	0.74	0.96	0.87	0.94	0.86
$\mu\text{g}/\text{m}^3$	biomass burning	0.85	0.23	0.89	0.24	0.72	0.62	0.78	0.53
$\mu\text{g}/\text{m}^3$	coal/fossil fuel combustion	0.91	0.69	0.95	0.62	0.88	0.77	0.93	0.91
$\mu\text{g}/\text{m}^3$	cooking markers	0.10	0.08	0.09	0.22	0.10	0.44	0.11	0.49
$\mu\text{g}/\text{m}^3$	dust	0.79	0.21	0.92	0.30	0.78	0.54	0.73	0.63
$\mu\text{g}/\text{m}^3$	biogenic SOA	0.87	0.36	0.84	0.59	0.80	0.63	0.94	0.90

## 4 Conclusions

This study presents a detailed and comprehensive analysis of  $\text{PM}_{2.5}$  oxidative potential and particle-bound ROS concentrations measured in winter 2016 and summer 2017 during the APHH-Beijing campaign at a central site in Beijing, China. Four acellular methods for measuring OP were applied, and correlated with providing a broad assessment of the oxidative properties of particles including particle-bound ROS concentrations, superoxide radical production and catalytic redox activity. We correlated the acellular assay responses with an extensive and comprehensive dataset including 107 additional atmospheric measurements (particle components, trace gases, meteorological parameters) to delineate chemical particle components and atmospheric processes and sources responsible for driving  $\text{PM}_{2.5}$  OP. Higher volume-normalised and mass-normalised OP values across all assays were observed in the winter compared to the summer. An inverse correlation was observed between  $\text{AA}_m$  and  $\text{DTT}_m$  with overall  $\text{PM}_{2.5}$  mass concentrations, i.e. days with higher  $\text{PM}_{2.5}$  mass concentrations have lower intrinsic OP values. This is likely due to an increase in OP-inactive material in high  $\text{PM}_{2.5}$  mass days, and/or a mass fraction that is at present undetermined and highlights that a focus on total PM exposure only does not necessarily capture accurately the oxidising properties and therefore certain toxicological effects of PM.

Univariate analysis with the additional 107 measurement parameters acquired during the APHH-Beijing campaign highlight significant assay-specific responses to chemical components of  $\text{PM}_{2.5}$ , as well as a seasonal difference in what components drive aerosol OP. It also highlights the importance of considering both volume-normalised and mass-normalised OP metrics when drawing conclusions on the role of chemical composition on OP, as assay correlations vary significantly between the two metrics. The data presented in this study illustrates that mass-normalised  $\text{OP}_m$  values provide a more nuanced picture of specific chemical components and sources that influence intrinsic OP, whereas many more correlations with  $\text{OP}_v$  values are observed, likely due to collinearity of many chemical components with overall  $\text{PM}_{2.5}$  mass concentrations driven by changes in meteorological conditions. Both metrics, mass-normalised  $\text{OP}_m$  as well as volume-normalised  $\text{OP}_v$ , are important to consider with  $\text{OP}_v$  a more relevant metric with respect to exposure and epidemiological studies, whereas  $\text{OP}_m$  provides more insight into what sources and what composition drives OP concentrations in particles. Furthermore,  $\text{OP}_m$  may allow easier

study and site inter-comparisons, ~~and reduces the impact on analyses of collinearity between PM<sub>2.5</sub> mass and concentrations of PM components due to meteorological factors.~~

The multivariate statistical analyses encapsulated the observations from the univariate analyses into comprehensive single models of OP relating to PM composition, and the inference from the univariate analyses that OP<sub>m</sub> measured by each assay is related to different compounds present in the particle was confirmed. ~~Variable~~It is clear from these differences that assay chemistry must contribute directly to its chemical selectivity, as the independent chemical measurements were given equal analytical weight with respect to each assay. The relationship between each assay and the independent measurements also confirmed that while there may exist a correlative relationship between an assay and non-redox active compounds such as *n*-alkanes or PAHs, the assay is more likely to be measuring either secondary oxidation products of these primary compounds or species co-emitted that contribute to particle OP. This represents a gap in the chemical analysis of these samples, and more detailed redox active compound speciation is required, especially for functionalised organics. Furthermore, variable selection of measurements and evaluation through multiple linear regression models indicated that OP<sub>m</sub> is well predicted by measurement panels characteristic of combustion sources, particularly (exhaust and non-exhaust) vehicle emissions, and biogenic SOA. ~~At present no single assay is completely representative of the totality of OP effects present in atmospheric PM. The comprehensive statistical analysis performed here shows This study demonstrates further that all four OP~~these commonly applied acellular assays are sensitive to a wide and differing range of different aerosol-chemical components, highlighting the advantage of using these assays as a they encompass multiple chemical components and sources ~~and atmospheric conditions and illustrate that with~~of aerosol into an integrated measurement. Further comprehensive work is needed to identify the current state of knowledge ~~none of these four assays can be disregarded with respect to their relevance for particle toxicity~~direct links between these OP assays and biological and toxicology data.

*Author Contributions.* SJC collated data, analysed filters for AA and DCFH, performed data analysis and interpretation and wrote the manuscript. KW performed univariate and multivariate statistical analysis, data interpretation and wrote the manuscript. BU, JW, ST and NS analysed filters for AA, DCFH, DTT and EPR respectively. TV provided XRF and additional data. AMS data were provided by YS. PAH data was provided by AE and AL. SOA tracer data was provided by DL, LL and PF. All other authors contributed to data analysis, interpretation and writing of the manuscript.

*Competing Interests.* The authors declare that they have no conflict of interest

*Special Issue Statement.* This article is part of the special issue “In-depth study of air pollution sources and processes within Beijing and its surrounding region (APHH-Beijing) (ACP/AMT inter-journal SI)

*Acknowledgements.* This work was funded by the European Research Council (ERC grant 279405), by the Natural Environment Research Council (NERC) (NE/K008218/1) and the Swiss National Science Foundation (200021\_192192 / 1).

This work has also received funding from the European Union's Horizon 2020 research and innovation programme through the EUROCHAMP-2020 Infrastructure Activity under grant agreement No. 730997. SSS additionally acknowledges support from the Swiss National Science Foundation (fellowship P2EZP2\_162258) and a 2017 LIFE PostDoc fellowship by the AXA Research Fund. We acknowledge the support from Pingqing Fu, Zifa Wang, Jie Li and Yele Sun from IAP for hosting the APHH-Beijing campaign at IAP. We thank Di Liu- from the University of Birmingham, Siyao Yue, Liangfang Wei, Hong Ren, Qiaorong Xie, Wanyu Zhao, Linjie Li, Ping Li, Shengjie Hou, Qingqing Wang from IAP, Rachel Dunmore and James Lee from the University of York, Kebin He and Xiaoting Cheng from Tsinghua University, and James Allan and Hugh Coe from the University of Manchester for providing logistic and scientific support for the field campaigns.

## References

- Acton, J., Hewitt, N., Huang, Z. and Wang, X.: APHH: Volatile organic compound (VOC) mixing ratios made at the IAP-Beijing site during the summer and winter campaigns. Centre for Environmental Data Analysis, 18.06.2020 <https://catalogue.ceda.ac.uk/uuid/de37c54e59a548ccb9f168ee724f3769>, 2018.
- Arangio, A. M., Tong, H., Socorro, J., Pöschl, U. and Shiraiwa, M.: Quantification of environmentally persistent free radicals and reactive oxygen species in atmospheric aerosol particles, *Atmos. Chem. Phys.*, 16(20), 13105–13119, doi:10.5194/acp-16-13105-2016, 2016.
- Atkinson, R. and Arey, J.: Mechanisms of the gas-phase reactions of aromatic hydrocarbons and pahas with oh and NO3 radicals, *Polycycl. Aromat. Compd.*, 27(1), 15–40, doi:10.1080/10406630601134243, 2007.
- Bates, J. T., Weber, R. J., Abrams, J., Verma, V., Fang, T., Klein, M., Strickland, M. J., Sarnat, S. E., Chang, H. H., Mulholland, J. A., Tolbert, P. E. and Russell, A. G.: Reactive Oxygen Species Generation Linked to Sources of Atmospheric Particulate Matter and Cardiorespiratory Effects, *Environ. Sci. Technol.*, 49(22), 13605–13612, doi:10.1021/acs.est.5b02967, 2015.
- Bates, J. T., Fang, T., Verma, V., Zeng, L., Weber, R. J., Tolbert, P. E., Abrams, J. Y., Sarnat, S. E., Klein, M., Mulholland, J. A. and Russell, A. G.: Review of Acellular Assays of Ambient Particulate Matter Oxidative Potential: Methods and Relationships with Composition, Sources, and Health Effects, *Environ. Sci. Technol.*, 53(8), 4003–4019, doi:10.1021/acs.est.8b03430, 2019.
- Biswas, S., Verma, V., Schauer, J. J., Cassee, F. R., Cho, A. K. and Sioutas, C.: Oxidative potential of semi-volatile and non volatile particulate matter (PM) from heavy-duty vehicles retrofitted with emission control technologies, *Environ. Sci. Technol.*, 43(10), 3905–3912, doi:10.1021/es9000592, 2009.
- Calas, A., Uzu, G., [Martins, J. M. F., Voisin, Di., Spadini, L., Lacroix, T. and Jaffrezo, J. L.: The importance of simulated lung fluid \(SLF\) extractions for a more relevant evaluation of the oxidative potential of particulate matter, \*Sci. Rep.\*, 7\(1\), 1–12, doi:10.1038/s41598-017-11979-3, 2017.](#)
- [Calas, A., Uzu, G., Kelly, F. J., Houdier, S., Martins, J. M. F., Thomas, F., Molton, F., Charron, A., Dunster, C., Oliete, A., Jacob, V., Besombes, J. L., Chevrier, F. and Jaffrezo, J. L.: Comparison between five acellular oxidative potential measurement](#)



- 865 assays performed with detailed chemistry on PM10 samples from the city of Chamonix (France), *Atmos. Chem. Phys.*, 18(11), 7863–7875, doi:10.5194/acp-18-7863-2018, 2018.
- Campbell, S., Stevanovic, S., Miljevic, B., Bottle, S. E., Ristovski, Z. D. and Kalberer, M.: Quantification of Particle-bound Organic Radicals in Secondary Organic Aerosol, *Environ. Sci. Technol.*, 53, 6729–6737, doi:10.1021/acs.est.9b00825, 2019a.
- 870 Campbell, S. J., Uttinger, B., Lienhard, D. M., Paulson, S. E., Shen, J., Griffiths, P. T., Stell, A. C. and Kalberer, M.: Development of a physiologically relevant online chemical assay to quantify aerosol oxidative potential, *Anal. Chem.*, 91, 13088–13095, doi:10.1021/acs.analchem.9b03282, 2019b.
- Campbell, S. J., Stevanovic, S., Miljevic, B., Bottle, S. E., Ristovski, Z. and Kalberer, M.: Quantification of Particle-Bound Organic Radicals in Secondary Organic Aerosol, *Environ. Sci. Technol.*, 53(12), 6729–6737, doi:10.1021/acs.est.9b00825, 2019b.
- 875 Charrier, J. G. and Anastasio, C.: Impacts of antioxidants on hydroxyl radical production from individual and mixed transition metals in a surrogate lung fluid, *Atmos. Environ.*, 45(40), 7555–7562, doi:10.1016/j.atmosenv.2010.12.021, 2011.
- Charrier, J. G. and Anastasio, C.: On dithiothreitol (DTT) as a measure of oxidative potential for ambient particles: evidence for the importance of soluble transition metals, *Atmos. Chem. Phys.*, 12(19), 9321–9333, doi:10.5194/acp-12-9321-2012, 2012.
- 880 Charrier, J. G., McFall, A. S., Richards-Henderson, N. K. and Anastasio, C.: Hydrogen peroxide formation in a surrogate lung fluid by transition metals and quinones present in particulate matter, *Environ. Sci. Technol.*, 48(12), 7010–7017, doi:10.1021/es501011w, 2014.
- Charrier, J. G., Richards-Henderson, N. K., Bein, K. J., McFall, A. S., Wexler, A. S. and Anastasio, C.: Oxidant production from source-oriented particulate matter - Part 1: Oxidative potential using the dithiothreitol (DTT) assay, *Atmos. Chem. Phys.*, 15(5), 2327–2340, doi:10.5194/acp-15-2327-2015, 2015.
- 885 Charrier, J. G., McFall, A. S., Vu, K. K. T., Baroi, J., Olea, C., Hasson, A. and Anastasio, C.: A bias in the “mass-normalized” DTT response – An effect of non-linear concentration-response curves for copper and manganese, *Atmos. Environ.*, 144, 325–334, doi:10.1016/j.atmosenv.2016.08.071, 2016.
- Cho, A. K., Sioutas, C., Miguel, A. H., Kumagai, Y., Schmitz, D. A., Singh, M., Eiguren-Fernandez, A. and Froines, J. R.: Redox activity of airborne particulate matter at different sites in the Los Angeles Basin, *Environ. Res.*, 99(1), 40–47, doi:10.1016/j.envres.2005.01.003, 2005.
- 890 Chung, M. Y., Lazaro, R. A., Lim, D., Jackson, J., Lyon, J., Rendulic, D. and Hasson, A. S.: Aerosol-borne quinones and reactive oxygen species generation by particulate matter extracts, *Environ. Sci. Technol.*, 40(16), 4880–4886, doi:10.1021/es0515957, 2006.
- Costa, D. L. and Dreher, K. L.: Bioavailable transition metals in particulate matter mediate cardiopulmonary injury in healthy and compromised animal models., *Environ. Health Perspect.*, 105 Suppl 5(September), 1053–1060, doi:10.1289/ehp.97105s51053, 1997.
- Delgado-Saborit, J. M., Alam, M. S., Godri Pollitt, K. J., Stark, C. and Harrison, R. M.: Analysis of atmospheric concentrations

of quinones and polycyclic aromatic hydrocarbons in vapour and particulate phases, *Atmos. Environ.*, 77, 974–982, doi:10.1016/j.atmosenv.2013.05.080, 2013.

Dellinger, B., Pryor, W. A., Cueto, R., Squadrito, G. L., Hegde, V. and Deutsch, W. A.: Role of free radicals in the toxicity of airborne fine particulate matter, *Chem. Res. Toxicol.*, 14(10), 1371–1377, doi:10.1021/tx010050x, 2001.

Ding, X., He, Q. F., Shen, R. Q., Yu, Q. Q., Zhang, Y. Q., Xin, J. Y., Wen, T. X. and Wang, X. M.: Spatial and seasonal variations of isoprene secondary organic aerosol in China: Significant impact of biomass burning during winter, *Sci. Rep.*, 6(20411), 1–10, doi:10.1038/srep20411, 2016.

Donaldson, K. and Tran, C. L.: Inflammation Caused By Particles and Fibers, *Inhal. Toxicol.*, 14(1), 5–27, doi:10.1080/089583701753338613, 2002.

Dou, J., Lin, P., Kuang, B. Y. and Yu, J. Z.: Reactive oxygen species production mediated by humic-like substances in atmospheric aerosols: Enhancement effects by pyridine, imidazole, and their derivatives, *Environ. Sci. Technol.*, 49(11), 6457–6465, doi:10.1021/es5059378, 2015.

Elzein, A., Dunmore, R. E., Ward, M. W., Hamilton, J. F. and Lewis, A. C.: Variability of polycyclic aromatic hydrocarbons and their oxidative derivatives in wintertime Beijing, China, *Atmos. Chem. Phys. Discuss.*, 1–28, doi:10.5194/acp-2019-120, 2019.

Elzein, A., Stewart, G. J., Swift, S. J., Nelson, B. S., Crilley, L. R., Alam, M. S., Reyes-villegas, E., Gadi, R., Harrison, R. M., Hamilton, J. F. and Lewis, A. C.: A comparison of PM<sub>2.5</sub>-bound polycyclic aromatic hydrocarbons in summer Beijing (China) and Delhi (India), *Atmos. Chem. Phys. Discuss.*, (August), 1–25, doi:https://doi.org/10.5194/acp-2020-770, 2020.

Eriksson, L., Byrne, T., Johansson, E., Trygg, J. and Vikstrom, C.: Multi-and megavariable data analysis basic principles and applications., 2013.

Fang, T., Verma, V., Guo, H., King, L. E., Edgerton, E. S. and Weber, R. J.: A semi-automated system for quantifying the oxidative potential of ambient particles in aqueous extracts using the dithiothreitol (DTT) assay: Results from the Southeastern Center for Air Pollution and Epidemiology (SCAPE), *Atmos. Meas. Tech.*, 8(1), 471–482, doi:10.5194/amt-8-471-2015, 2015.

Fang, T., Verma, V., Bates, J. T., Abrams, J., Klein, M., Strickland, M. J., Sarnat, S. E., Chang, H. H., Mulholland, J. A., Tolbert, P. E., Russell, A. G. and Weber, R. J.: Oxidative potential of ambient water-soluble PM<sub>2.5</sub> in the southeastern United States : contrasts in sources and health associations between ascorbic acid (AA) and dithiothreitol (DTT) assays, , 3865–3879, doi:10.5194/acp-16-3865-2016, 2016.

Feng, B., Li, L., Xu, H., Wang, T., Wu, R., Chen, J., Zhang, Y., Liu, S., Ho, S. S. H., Cao, J. and Huang, W.: PM<sub>2.5</sub>-bound polycyclic aromatic hydrocarbons (PAHs) in Beijing: Seasonal variations, sources, and risk assessment, *J. Environ. Sci. (China)*, 77, 11–19, doi:10.1016/j.jes.2017.12.025, 2019.

Fuller, S. J., Wragg, F. P. H., Nutter, J. and Kalberer, M.: Comparison of on-line and off-line methods to quantify reactive oxygen species (ROS) in atmospheric aerosols, *Atmos. Environ.*, 92, 97–103, doi:10.1016/j.atmosenv.2014.04.006, 2014.

Gallimore, P. J., Mahon, B. M., Wragg, F. P. H., Fuller, S. J., Giorio, C., Kourtchev, I. and Kalberer, M.: Multiphase composition changes and reactive oxygen species formation during limonene oxidation in the new Cambridge Atmospheric

- Simulation Chamber (CASC), *Atmos. Chem. Phys.*, 17, 9853–9868, doi:10.5194/acp-2017-186, 2017.
- 935 Gao, J., Tian, H., Cheng, K., Lu, L., Wang, Y., Wu, Y., Zhu, C., Liu, K., Zhou, J., Liu, X., Chen, J. and Hao, J.: Seasonal and spatial variation of trace elements in multi-size airborne particulate matters of Beijing, China: Mass concentration, enrichment characteristics, source apportionment, chemical speciation and bioavailability, *Atmos. Environ.*, 99, 257–265, doi:10.1016/j.atmosenv.2014.08.081, 2014.
- Gehling, W. and Dellinger, B.: Environmentally persistent free radicals and their lifetimes in PM<sub>2.5</sub>, *Environ. Sci. Technol.*, 47(15), 8172–8178, doi:10.1021/es401767m, 2013.
- 940 Gehling, W., Khachatryan, L. and Dellinger, B.: Hydroxyl radical generation from environmentally persistent free radicals (EPFRs) in PM<sub>2.5</sub>, *Environ. Sci. Technol.*, 48(8), 4266–4272, doi:10.1021/es401770y, 2014.
- Ghio, A. J., Stonehuerner, J., Dailey, L. A. and Carter, J. D.: Metals associated with both the water-soluble and insoluble fractions of an ambient air pollution particle catalyze an oxidative stress, *Inhal. Toxicol.*, 11(1), 37–49, doi:10.1080/089583799197258, 1999.
- 945 Ghio, A. J., Carraway, M. S. and Madden, M. C.: Composition of air pollution particles and oxidative stress in cells, tissues, and living systems, *J. Toxicol. Environ. Heal. - Part B Crit. Rev.*, 15(1), 1–21, doi:10.1080/10937404.2012.632359, 2012.
- Godri, K. J., Harrison, R. M., Evans, T., Baker, T., Dunster, C., Mudway, I. S. and Kelly, F. J.: Increased oxidative burden associated with traffic component of ambient particulate matter at roadside and Urban background schools sites in London, *PLoS One*, 6(7), doi:10.1371/journal.pone.0021961, 2011.
- 950 Hart, J. E., Liao, X., Hong, B., Puett, R. C., Yanosky, J. D., Suh, H., Kioumourtoglou, M. A., Spiegelman, D. and Laden, F.: The association of long-term exposure to PM<sub>2.5</sub> on all-cause mortality in the Nurses' Health Study and the impact of measurement-error correction, *Environ. Heal.*, 14(1), 38, doi:10.1186/s12940-015-0027-6, 2015.
- Hasson, A. S. and Paulson, S. E.: An investigation of the relationship between gas-phase and aerosol-borne hydroperoxides in urban air, *J. Aerosol Sci.*, 34(4), 459–468, doi:10.1016/S0021-8502(03)00002-8, 2003.
- 955 He, L. Y., Hu, M., Huang, X. F., Zhang, Y. H. and Tang, X. Y.: Seasonal pollution characteristics of organic compounds in atmospheric fine particles in Beijing, *Sci. Total Environ.*, 359(1–3), 167–176, doi:10.1016/j.scitotenv.2005.05.044, 2006.
- Hewitt, C. N. and Kok, G. L.: Formation and occurrence of organic hydroperoxides in the troposphere: Laboratory and field observations, *J. Atmos. Chem.*, 12(2), 181–194, doi:10.1007/BF00115779, 1991.
- Hung, H. F. and Wang, C.-S.: Experimental determination of reactive oxygen species in Taipei aerosols, *J. Aerosol Sci.*, 960 32(10), 1201–1211, doi:10.1016/S0021-8502(01)00051-9, 2001.
- Janssen, N. A. H., Yang, A., Strak, M., Steenhof, M., Hellack, B., Gerlofs-Nijland, M. E., Kuhlbusch, T., Kelly, F., Harrison, R., Brunekreef, B., Hoek, G. and Cassee, F.: Oxidative potential of particulate matter collected at sites with different source characteristics, *Sci. Total Environ.*, 472, 572–581, doi:10.1016/j.scitotenv.2013.11.099, 2014.
- Jedynska, A., Hoek, G., Wang, M., Yang, A., Eeftens, M., Cyrys, J., Keuken, M., Ampe, C., Beelen, R., Cesaroni, G., 965 Forastiere, F., Cirach, M., de Hoogh, K., De Nazelle, A., Nystad, W., Akhlaghi, H. M., Declercq, C., Stempfelet, M., Eriksen, K. T., Dimakopoulou, K., Lanki, T., Meliefste, K., Nieuwenhuijsen, M., Yli-Tuomi, T., Raaschou-Nielsen, O., Janssen, N. A.

H., Brunekreef, B. and Kooter, I. M.: Spatial variations and development of land use regression models of oxidative potential in ten European study areas, *Atmos. Environ.*, 150, 24–32, doi:10.1016/j.atmosenv.2016.11.029, 2017.

Kelly, F. J.: Oxidative stress: ~~its~~<sup>its</sup> role in air pollution and adverse health effects, *Occup. Environ. Med.*, 60(8), 612–616, doi:10.1136/oem.60.8.612, 2003.

Knaapen, A. M., Borm, P. J. A., Albrecht, C. and Schins, R. P. F.: Inhaled particles and lung cancer. Part A: Mechanisms, *Int. J. Cancer*, 109(6), 799–809, doi:10.1002/ijc.11708, 2004.

Laden, F., Schwartz, J., Speizer, F. E. and Dockery, D. W.: Reduction in fine particulate air pollution and mortality: Extended follow-up of the Harvard Six Cities Study, *Am. J. Respir. Crit. Care Med.*, 173(6), 667–672, doi:10.1164/rccm.200503-443OC, 2006.

Laing, S., Wang, G., Briazova, T., Zhang, C., Wang, A., Zheng, Z., Gow, A., Chen, A. F., Rajagopalan, S., Chen, L. C., Sun, Q. and Zhang, K.: Airborne particulate matter selectively activates endoplasmic reticulum stress response in the lung and liver tissues, *Am. J. Physiol. - Cell Physiol.*, 299(4), 736–749, doi:10.1152/ajpcell.00529.2009, 2010.

Lelieveld, J., Pozzer, A., Pöschl, U., Fnais, M., Haines, A. and Münzel, T.: Loss of life expectancy from air pollution compared to other risk factors: a worldwide perspective, *Cardiovasc. Res.*, 116(11), 1910–1917, doi:10.1093/cvr/cvaa025, 2020.

Lepeule, J., Laden, F., Dockery, D. and Schwartz, J.: Chronic exposure to fine particles and mortality: An extended follow-up of the Harvard six cities study from 1974 to 2009, *Environ. Health Perspect.*, 120(7), 965–970, doi:10.1289/ehp.1104660, 2012.

Levy, J. I., Diez, D., Dou, Y., Barr, C. D. and Dominici, F.: A meta-analysis and multisite time-series analysis of the differential toxicity of major fine particulate matter constituents, *Am. J. Epidemiol.*, 175(11), 1091–1099, doi:10.1093/aje/kwr457, 2012.

Li, N., Hao, M., Phalen, R. F., Hinds, W. C. and Nel, A. E.: Particulate air pollutants and asthma: A paradigm for the role of oxidative stress in PM-induced adverse health effects, *Clin. Immunol.*, 109(3), 250–265, doi:10.1016/j.clim.2003.08.006, 2003.

Li, N., Xia, T. and Nel, A. E.: The Role of Oxidative Stress in Ambient Particulate Matter Induced Lung Diseases and its Implications in the Toxicity of Engineered Nanoparticles, *Free Radic. Bio. Med.*, 9(44), 1689–1699, doi:10.1038/mp.2011.182, 2008.

Li, X., Jiang, L., Bai, Y., Yang, Y., Liu, S., Chen, X., Xu, J., Liu, Y., Wang, Y., Guo, X., Wang, Y. and Wang, G.: Wintertime aerosol chemistry in Beijing during haze period: Significant contribution from secondary formation and biomass burning emission, *Atmos. Res.*, 218(October 2018), 25–33, doi:10.1016/j.atmosres.2018.10.010, 2019.

Li, Y.: Observational accuracy of sunrise and sunset times in the sixth century China, *Chinese J. Astron. Astrophys.*, 6(5), doi:10.1088/1009-9271/6/5/16, 2006.

Liang, L., Engling, G., Duan, F., Cheng, Y. and He, K.: Characteristics of 2-methyltetrols in ambient aerosol in Beijing, China, *Atmos. Environ.*, 59, 376–381, doi:10.1016/j.atmosenv.2012.05.052, 2012.

Lim, Y. Bin and Ziemann, P. J.: Products and mechanism of secondary organic aerosol formation from reactions of n-alkanes with OH radicals in the presence of NO<sub>x</sub>, *Environ. Sci. Technol.*, 39(23), 9229–9236, doi:10.1021/es051447g, 2005.

Liu, D., Harrison, R. M., Vu, T., Xu, J., Shi, Z., Li, L., Sun, Y. and Fu, P.: Estimation of biogenic and anthropogenic precursor contributions to secondary organic aerosol in Beijing using molecular tracers, *Prep.*, 2020.

Liu, Q., Baumgartner, J., Zhang, Y., Liu, Y., Sun, Y. and Zhang, M.: Oxidative potential and inflammatory impacts of source apportioned ambient air pollution in Beijing, *Environ. Sci. Technol.*, 48(21), 12920–12929, doi:10.1021/es5029876, 2014.

1005 Liu, W. J., Xu, Y. S., Liu, W. X., Liu, Q. Y., Yu, S. Y., Liu, Y., Wang, X. and Tao, S.: Oxidative potential of ambient PM<sub>2.5</sub> in the coastal cities of the Bohai Sea, northern China: Seasonal variation and source apportionment, *Environ. Pollut.*, 236, 514–528, doi:10.1016/j.envpol.2018.01.116, 2018.

Ma, Y., Cheng, Y., Qiu, X., Cao, G., Fang, Y., Wang, J., Zhu, T., Yu, J. and Hu, D.: Sources and oxidative potential of water-soluble humic-like substances (HULISWS) in fine particulate matter (PM<sub>2.5</sub>) in Beijing, *Atmos. Chem. Phys.*, 18(8), 5607–5617, doi:10.5194/acp-18-5607-2018, 2018.

1010 McWhinney, R. D., Badali, K., Liggio, J., Li, S. M. and Abbatt, J. P. D.: Filterable redox cycling activity: A comparison between diesel exhaust particles and secondary organic aerosol constituents, *Environ. Sci. Technol.*, 47(7), 3362–3369, doi:10.1021/es304676x, 2013a.

McWhinney, R. D., Zhou, S. and Abbatt, J. P. D.: Naphthalene SOA: Redox activity and naphthoquinone gas-particle partitioning, *Atmos. Chem. Phys.*, 13(19), 9731–9744, doi:10.5194/acp-13-9731-2013, 2013b.

1015 Meng, Z. and Zhang, Q.: Oxidative damage of dust storm fine particles instillation on lungs, hearts and livers of rats, *Environ. Toxicol. Pharmacol.*, 22(3), 277–282, doi:10.1016/j.etap.2006.04.005, 2006.

Miller, M. R., Borthwick, S. J., Shaw, C. A., McLean, S. G., McClure, D., Mills, N. L., Duffin, R., Donaldson, K., Megson, I. L., Hadoke, P. W. F. and Newby, D. E.: Direct impairment of vascular function by diesel exhaust particulate through reduced bioavailability of endothelium-derived nitric oxide induced by superoxide free radicals, *Environ. Health Perspect.*, 117(4), 611–616, doi:10.1289/ehp.0800235, 2009.

Miyata, R. and van Eeden, S. F.: The innate and adaptive immune response induced by alveolar macrophages exposed to ambient particulate matter, *Toxicol. Appl. Pharmacol.*, 257(2), 209–226, doi:10.1016/j.taap.2011.09.007, 2011.

Moorthy, B., Chu, C. and Carlin, D. J.: Polycyclic aromatic hydrocarbons: From metabolism to lung cancer, *Toxicol. Sci.*, 145(1), 5–15, doi:10.1093/toxsci/kfv040, 2015.

1025 Müller, L., Reinnig, M. C., Naumann, K. H., Saathoff, H., Mentel, T. F., Donahue, N. M. and Hoffmann, T.: Formation of 3-methyl-1,2,3-butanetricarboxylic acid via gas phase oxidation of pinonic acid - A mass spectrometric study of SOA aging, *Atmos. Chem. Phys.*, 12(3), 1483–1496, doi:10.5194/acp-12-1483-2012, 2012.

Naes, T. and Martens, H.: Principal component regression in NIR analysis: viewpoints, background details and selection of components, *J. Chemom.*, 2(2), 155–167, 1988.

1030 Ntziachristos, L., Froines, J. R., Cho, A. K. and Sioutas, C.: Relationship between redox activity and chemical speciation of size-fractionated particulate matter, *Part. Fibre Toxicol.*, 4, 1–12, doi:10.1186/1743-8977-4-5, 2007.

Oberdorster, G., Ferin, J., Gelein, R., Soderholm, S. C. and Finkelstein, J.: Role of the alveolar macrophage in lung injury: Studies with ultrafine particles, *Environ. Health Perspect.*, 97, 193–199, doi:10.1289/ehp.97-1519541, 1992.

- 1035 Øvrevik, J., Refsnes, M., Låg, M., Holme, J. A. and Schwarze, P. E.: Activation of proinflammatory responses in cells of the airway mucosa by particulate matter: Oxidant- and non-oxidant-mediated triggering mechanisms, *Biomolecules*, 5(3), 1399–1440, doi:10.3390/biom5031399, 2015.
- Paatero, P. and Tapper, U.: Postive Matrix Factorisation: A non-negative factor model with optimal utilization of error estimates of data values, *Environmetrics*, 5(2), 111–126, 1994.
- 1040 Panagi, M., Fleming, Z. L., Monks, P. S., Ashfold, M. J., Wild, O., Hollaway, M., Zhang, Q., Squires, F. A. and Vande Hey, J. D.: Investigating the regional contributions to air pollution in Beijing: A dispersion modelling study using CO as a tracer, *Atmos. Chem. Phys.*, 20(5), 2825–2838, doi:10.5194/acp-20-2825-2020, 2020.
- Pant, P., Baker, S. J., Shukla, A., Maikawa, C., Godri Pollitt, K. J. and Harrison, R. M.: The PM10 fraction of road dust in the UK and India: Characterization, source profiles and oxidative potential, *Sci. Total Environ.*, 530–531, 445–452, doi:10.1016/j.scitotenv.2015.05.084, 2015.
- 1045 Paulson, S. E., Gallimore, P. J., Kuang, X. M., Chen, J. R., Kalberer, M. and Gonzalez, D. H.: A light-driven burst of hydroxyl radicals dominates oxidation chemistry in newly activated cloud droplets, *Sci. Adv.*, 5(5), 1–8, doi:10.1126/sciadv.aav7689, 2019.
- Pernigotti, D., Belis, C. A. and Spano, L.: SPECIEUROPE: The European data base for PM source profiles., *Atmos. Pollut. Res.*, 7(2), 307–314, 2016.
- 1050 Platt, S. M., Haddad, I. El, Pieber, S. M., Huang, R. J., Zardini, A. A., Clairotte, M., Suarez-Bertoa, R., Barmet, P., Pfaffenberger, L., Wolf, R., Slowik, J. G., Fuller, S. J., Kalberer, M., Chirico, R., Dommen, J., Astorga, C., Zimmermann, R., Marchand, N., Hellebust, S., Temime-Roussel, B., Baltensperger, U. and Prévôt, A. S. H.: Two-stroke scooters are a dominant source of air pollution in many cities, *Nat. Commun.*, 5(May), 1–7, doi:10.1038/ncomms4749, 2014.
- 1055 Pope, C. A. and Dockery, D. W.: Health effects of fine particulate air pollution: Lines that connect, *J. Air Waste Manag. Assoc.*, 56(6), 709–742, doi:10.1080/10473289.2006.10464485, 2006.
- Presto, A. A., Miracolo, M. A., Donahue, N. M. and Robinson, A. L.: Secondary organic aerosol formation from high-NO<sub>x</sub> Photo-oxidation of low volatility precursors: N-alkanes, *Environ. Sci. Technol.*, 44(6), 2029–2034, doi:10.1021/es903712r, 2010.
- 1060 Puthussery, J. V., Singh, A., Rai, P., Bhattu, D., Kumar, V., Vats, P., Furger, M., Rastogi, N., Slowik, J. G., Ganguly, D., Prevot, A. S. H., Tripathi, S. N. and Verma, V.: Real-Time Measurements of PM 2.5 Oxidative Potential Using a Dithiothreitol Assay in Delhi, India , *Environ. Sci. Technol. Lett.*, doi:10.1021/acs.estlett.0c00342, 2020.
- Risom, L., Møller, P. and Loft, S.: Oxidative stress-induced DNA damage by particulate air pollution, *Mutat-Res., Res. - Fundam. Mol. Mech. Mutagen.*, 592(1–2), 119–137, doi:10.1016/j.mrfmmm.2005.06.012, 2005.
- 1065 Saffari, A., Daher, N., Shafer, M. M., Schauer, J. J. and Sioutas, C.: Seasonal and spatial variation in reactive oxygen species activity of quasi-ultrafine particles (PM<sub>0.25</sub>) in the Los Angeles metropolitan area and its association with chemical composition, *Atmos. Environ.*, 79, 566–575, doi:10.1016/j.atmosenv.2013.07.058, 2013.
- Saffari, A., Daher, N., Shafer, M. M., Schauer, J. J. and Sioutas, C.: Seasonal and spatial variation in dithiothreitol (DTT)

activity of quasi-ultrafine particles in the Los Angeles Basin and its association with chemical species, *J. Environ. Sci. Heal. - Part A Toxic/Hazardous Subst. Environ. Eng.*, 49(4), 441–451, doi:10.1080/10934529.2014.854677, 2014.

Schauer, J. J., Kleeman, M. J., Cass, G. R. and Simoneit, B. R. T.: Measurement of emissions from air pollution sources. 2. C1 through C30 organic compounds from medium duty diesel trucks, *Environ. Sci. Technol.*, 33(10), 1578–1587, doi:10.1021/es980081n, 1999.

See, S. W., Wang, Y. H. and Balasubramanian, R.: Contrasting reactive oxygen species and transition metal concentrations in combustion aerosols, *Environ. Res.*, 103(3), 317–324, doi:10.1016/j.envres.2006.08.012, 2007.

Shen, H. and Anastasio, C.: ~~Formation~~A comparison of hydroxyl radical ~~from San Joaquin Valley particles extracted and hydrogen peroxide generation in a cell-free surrogate lung fluid ambient particle extracts and laboratory metal solutions~~, *Atmos. Chem. Phys.*, 11(18), 9671–9682 *Environ.*, 46(530), 665–668, doi:10.5194/acp-11-9671-1016/j.atmosenv.2011.2011.10.006, 2012.

Shen, H. and Anastasio, C.: ~~A comparison of hydroxyl radical and hydrogen peroxide generation in ambient particle extracts and laboratory metal solutions~~, *Atmos. Environ.*, 46(530), 665–668, doi:10.1016/j.atmosenv.2011.10.006, 2012.

Shen, H., Barakat, A. I. and Anastasio, C.: ~~Generation of hydrogen peroxide from San Joaquin Valley particles in a cell-free solution~~, *Atmos. Chem. Phys.*, 11(2), 753–765, doi:10.5194/acp-11-753-2011, 2011.

Shen, R., Liu, Z., Liu, Y., Wang, L., Li, D., Wang, Y., Wang, G., Bai, Y. and Li, X.: Typical polar organic aerosol tracers in PM2.5 over the North China Plain: Spatial distribution, seasonal variations, contribution and sources, *Chemosphere*, 209, 758–766, doi:10.1016/j.chemosphere.2018.06.133, 2018.

Shi, Z., Vu, T., Kotthaus, S., Harrison, R. M., Grimmond, S., Yue, S., Zhu, T., Lee, J., Han, Y., Demuzere, M., Dunmore, R. E., Ren, L., Liu, D., Wang, Y., Wild, O., Allan, J., Acton, W. J., Barlow, J., Barratt, B., Beddows, D., Bloss, W. J., Calzolari, G., Carruthers, D., Carslaw, D. C., Chan, Q., Chatzidiakou, L., Chen, Y., Crilley, L., Coe, H., Dai, T., Doherty, R., Duan, F., Fu, P., Ge, B., Ge, M., Guan, D., Hamilton, J. F., He, K., Heal, M., Heard, D., Hewitt, C. N., Hollaway, M., Hu, M., Ji, D., Jiang, X., Jones, R., Kalberer, M., Kelly, F. J., Kramer, L., Langford, B., Lin, C., Lewis, A. C., Li, J., Li, W., Liu, H., Liu, J., Loh, M., Lu, K., Lucarelli, F., Mann, G., Mcfiggans, G., Miller, M. R., Mills, G., Monk, P., Nemitz, E., Ouyang, B., Palmer, P. I., Percival, C., Popoola, O., Reeves, C., Rickard, A. R., Shao, L., Shi, G., Spracklen, D., Stevenson, D., Sun, Y., Sun, Z., Tao, S., Tong, S., Wang, Q., Wang, W., Wang, X., Wang, X., Wang, Z., Wei, L., Whalley, L., Wu, X., Wu, Z., Xie, P., Yang, F., Zhang, Q., Zhang, Y., Zhang, Y. and Zheng, M.: Introduction to the special issue “ In-depth study of air pollution sources and processes within Beijing and its surrounding region , 7519–7546, 2019.

Shinyashiki, M., Eiguren-Fernandez, A., Schmitz, D. A., Di Stefano, E., Li, N., Linak, W. P., Cho, S. H., Froines, J. R. and Cho, A. K.: Electrophilic and redox properties of diesel exhaust particles, *Environ. Res.*, 109(3), 239–244, doi:10.1016/j.envres.2008.12.008, 2009.

Steimer, S., Patton, D., Vu, T., Panagi, M., Monks, P., Harrison, R., Fleming, Z., Shi, Z. and Kalberer, M.: Seasonal Differences in the Composition of Organic Aerosols in Beijing: a Study by Direct Infusion Ultrahigh Resolution Mass Spectrometry, *Atmos. Chem. Phys. Discuss.*, (January), 1–26, doi:10.5194/acp-2019-1009, 2020.

Steimer, S. S., Delvaux, A., Campbell, S. J., Gallimore, P. J., Grice, P., Howe, D. J., Pitton, D., Claeys, M., Hoffmann, T. and Kalberer, M.: Synthesis and characterisation of peroxydic acids as proxies for highly oxygenated molecules (HOMs) in secondary organic aerosol, *Atmos. Chem. Phys.*, 18(15), 10973–10983, doi:10.5194/acp-18-10973-2018, 2018.

Subramanian, R., Donahue, N. M., Bernardo-Bricker, A., Rogge, W. F. and Robinson, A. L.: Contribution of motor vehicle emissions to organic carbon and fine particle mass in Pittsburgh, Pennsylvania: Effects of varying source profiles and seasonal trends in ambient marker concentrations, *Atmos. Environ.*, 40(40), 8002–8019, doi:10.1016/j.atmosenv.2006.06.055, 2006.

Tan, W. C., Qiu, D., Liam, B. L., Ng, T. P., Lee, S. H., Van Eeden, S. F., D’Yachkova, Y. and Hogg, J. C.: The human bone marrow response to acute air pollution caused by forest fires, *Am. J. Respir. Crit. Care Med.*, 161(4 I), 1213–1217, doi:10.1164/ajrccm.161.4.9904084, 2000.

Tao, F., Gonzalez-Flecha, B. and Kobzik, L.: Reactive oxygen species in pulmonary inflammation by ambient particulates, *Free Radic. Biol. Med.*, 35(4), 327–340, doi:10.1016/S0891-5849(03)00280-6, 2003.

Tapparo, A., Di Marco, V., Badocco, D., D’Aronco, S., Soldà, L., Pastore, P., Mahon, B. M., Kalberer, M. and Giorio, C.: Formation of metal-organic ligand complexes affects solubility of metals in airborne particles at an urban site in the Po valley, *Chemosphere*, 241, 1–13, doi:10.1016/j.chemosphere.2019.125025, 2020.

Tong, H., Arangio, A. M., Lakey, P. S. J., Berkemeier, T., Liu, F., Kampf, C. J., Brune, W. H., Pöschl, U. and Shiraiwa, M.: Hydroxyl radicals from secondary organic aerosol decomposition in water, *Atmos. Chem. Phys.*, 16(3), 1761–1771, doi:10.5194/acp-16-1761-2016, 2016.

Tong, H., Lakey, P. S. J., Arangio, A. M., Socorro, J., Kampf, C. J., Berkemeier, T., Brune, W. H., Pöschl, U. and Shiraiwa, M.: Reactive oxygen species formed in aqueous mixtures of secondary organic aerosols and mineral dust influencing cloud chemistry and public health in the Anthropocene, *Faraday Discuss.*, 200, 251–270, doi:10.1039/c7fd00023e, 2017.

Tong, H., Lakey, P. S. J., Arangio, A. M., Socorro, J., Shen, F., Lucas, K., Brune, W. H., Pöschl, U. and Shiraiwa, M.: Reactive Oxygen Species Formed by Secondary Organic Aerosols in Water and Surrogate Lung Fluid, *Environ. Sci. Technol.*, 52, 11642–11651, doi:10.1021/acs.est.8b03695, 2018.

Tuet, W. Y., Chen, Y., Xu, L., Fok, S., Gao, D., Weber, R. J. and Ng, N. L.: Chemical oxidative potential of secondary organic aerosol (SOA) generated from the photooxidation of biogenic and anthropogenic volatile organic compounds, , 839–853, doi:10.5194/acp-17-839-2017, 2017.

Valko, M., Morris, H. and Cronin, M. T. D.: Metals, Toxicity and Oxidative Stress, *Curr. Med. Chem.*, 12(10), 1161–1208, 2005.

Venkatachari, P. and Hopke, P. K.: Development and laboratory testing of an automated monitor for the measurement of atmospheric particle-bound reactive oxygen species (ROS), *Aerosol Sci. Technol.*, 42(8), 629–635, 2008.

Venkatachari, P., Hopke, P. K., Grover, B. D. and Eatough, D. J.: Measurement of particle-bound reactive oxygen species in rubidoux aerosols, *J. Atmos. Chem.*, 50(1), 49–58, doi:10.1007/s10874-005-1662-z, 2005.

Verma, V., Pakbin, P., Cheung, K. L., Cho, A. K., Schauer, J. J., Shafer, M. M., Kleinman, M. T. and Sioutas, C.: Physicochemical and oxidative characteristics of semi-volatile components of quasi-ultrafine particles in an urban atmosphere,



Atmos. Environ., 45(4), 1025–1033, doi:10.1016/j.atmosenv.2010.10.044, 2011.

Verma, V., Fang, T., Guo, H., King, L., Bates, J. T., Peltier, R. E., Edgerton, E., Russell, A. G. and Weber, R. J.: Reactive oxygen species associated with water-soluble PM<sub>2.5</sub> in the southeastern United States: Spatiotemporal trends and source apportionment, *Atmos. Chem. Phys.*, 14(23), 12915–12930, doi:10.5194/acp-14-12915-2014, 2014.

Verma, V., Wang, Y., El-Affif, R., Fang, T., Rowland, J., Russell, A. G. and Weber, R. J.: Fractionating ambient humic-like substances (HULIS) for their reactive oxygen species activity - Assessing the importance of quinones and atmospheric aging, *Atmos. Environ.*, 120, 351–359, doi:10.1016/j.atmosenv.2015.09.010, 2015a.

Verma, V., Fang, T., Xu, L., Peltier, R. E., Russell, A. G., Ng, N. L. and Weber, R. J.: Organic aerosols associated with the generation of reactive oxygen species (ROS) by water-soluble PM<sub>2.5</sub>, *Environ. Sci. Technol.*, 49(7), 4646–4656, doi:10.1021/es505577w, 2015b.

Wang, G., Cheng, S., Wei, W., Zhou, Y., Yao, S. and Zhang, H.: Characteristics and source apportionment of VOCs in the suburban area of Beijing, China, *Atmos. Pollut. Res.*, 7(4), 711–724, doi:10.1016/j.apr.2016.03.006, 2016.

Wang, H., Li, Z., Lv, Y., Zhang, Y., Xu, H., Guo, J. and Goloub, P.: Determination and climatology of diurnal cycle of atmospheric mixing layer height over Beijing 2013&#8211;2018: Lidar measurements and implication for airpollution, *Atmos. Chem. Phys.*, 1–25, doi:10.5194/acp-2020-175, 2020a.

Wang, J., Jiang, H., Jiang, H., Mo, Y., Geng, X., Li, J., Mao, S., Bualert, S., Ma, S., Li, J. and Zhang, G.: Source apportionment of water-soluble oxidative potential in ambient total suspended particulate from Bangkok: Biomass burning versus fossil fuel combustion, *Atmos. Environ.*, 235(May), 117624, doi:10.1016/j.atmosenv.2020.117624, 2020b.

Wang, Q., He, X., Zhou, M., Huang, D., Qiao, L., Zhu, S., Ma, Y., Wang, H., Li, L., Huang, C., Huang, X. H. H., Xu, W., Worsnop, D. R., Goldstein, A. H., Guo, H. and Yu, J. Z.: Hourly Measurements of Organic Molecular Markers in Urban Shanghai, China: Primary Organic Aerosol Source Identification and Observation of Cooking Aerosol Aging, *ACS Earth Sp. Chem.*, doi:10.1021/acsearthspacechem.0c00205, 2020c.

Wang, Y., Plewa, M. J., Mukherjee, U. K. and Verma, V.: Assessing the cytotoxicity of ambient particulate matter (PM) using Chinese hamster ovary (CHO) cells and its relationship with the PM chemical composition and oxidative potential, *Atmos. Environ.*, 179(September 2017), 132–141, doi:10.1016/j.atmosenv.2018.02.025, 2018.

Whalley, L. K., Slater, E. J., Woodward-Massey, R., Ye, C., Lee, J. D., Squires, F., Hopkins, J. R., Dunmore, R. E., Shaw, M., Hamilton, J. F., Lewis, A. C., Mehra, A., Worrall, S. D., Bacak, A., Bannan, T. J., Coe, H., Ouyang, B., Jones, R. L., Crilley, L. R., Kramer, L. J., Bloss, W. J., Vu, T., Kotthaus, S., Grimmond, S., Sun, Y., Xu, W., Yue, S., Ren, L., Joe, W., Acton, F., Hewitt, C. N., Wang, X., Fu, P., Heard, D. E. and Whalley, L.: Evaluating the sensitivity of radical chemistry and ozone formation to ambient VOCs and NO<sub>x</sub> in Beijing, , (x), 1–41, doi:10.5194/acp-2020-785, 2020.

World Health Organisation: Ambient Air Pollution: A Global Assessment of Exposure and Burden of Disease., 2016.

Wragg, F. P. H., Fuller, S. J., Freshwater, R., Green, D. C., Kelly, F. J. and Kalberer, M.: An automated online instrument to quantify aerosol-bound reactive oxygen species (ROS) for ambient measurement and health-relevant aerosol studies, *Atmos. Meas. Tech.*, 9(10), 4891–4900, doi:10.5194/amt-9-4891-2016, 2016.

- Xu, J., Liu, D., Wu, X., Vu, T. V., Zhang, Y. Z., Fu, P., Sun, Y., Xu, W., Ji, D., Harrison, R. M. and Shi, Z.: Source Apportionment of Fine Aerosol at an Urban Site of Beijing Using a Chemical Mass Balance Model, *Prep.*, 2020a.
- Xu, J., Hu, W., Liang, D. and Gao, P.: Technology Photochemical impacts on the toxicity of PM<sub>2.5</sub>, *Crit. Rev. Environ. Sci. Technol.*, 0(0), 1–27, doi:10.1080/10643389.2020.1816126, 2020b.
- 1175 Yang, A., Wang, M., Eeftens, M., Beelen, R., Dons, E., Leseman, D. L. A. C., Brunekreef, B., Cassee, F. R., Janssen, N. A. H. and Hoek, G.: Spatial variation and land use regression modeling of the oxidative potential of fine particles, *Environ. Health Perspect.*, 123(11), 1187–1192, doi:10.1289/ehp.1408916, 2015.
- Yu, L., Wang, G., Zhang, R., Zhang, L., Song, Y., Wu, B., Li, X., An, K. and Chu, J.: Characterization and source apportionment of PM<sub>2.5</sub> in an urban environment in Beijing, *Aerosol Air Qual. Res.*, 13(2), 574–583, doi:10.4209/aaqr.2012.07.0192, 2013.
- 1180 Yu, S. Y., Liu, W. J., Xu, Y. S., Yi, K., Zhou, M., Tao, S. and Liu, W. X.: Characteristics and oxidative potential of atmospheric PM<sub>2.5</sub> in Beijing: Source apportionment and seasonal variation, *Sci. Total Environ.*, 650, 277–287, doi:10.1016/j.scitotenv.2018.09.021, 2019.
- Zhao, H., Zheng, Y. and Li, C.: Spatiotemporal distribution of PM<sub>2.5</sub> and O<sub>3</sub> and their interaction during the summer and winter seasons in Beijing, China, *Sustain.*, 10(12), doi:10.3390/su10124519, 2018.
- 1185 Zheng, M., Salmon, L. G., Schauer, J. J., Zeng, L., Kiang, C. S., Zhang, Y. and Cass, G. R.: Seasonal trends in PM<sub>2.5</sub> source contributions in Beijing, China, *Atmos. Environ.*, 39(22), 3967–3976, doi:10.1016/j.atmosenv.2005.03.036, 2005.